# Design a single channel EEG system and processing the corresponding signals using HMM

By

Hamza F. Altakroury

Shehdeh A.M. Zahdeh

Supervisor
Dr. Hashem Tamimi
Eng. Ali Amro

Submitted to
College of Engineering and Technology
Electrical and Computer Systems Department

Palestine Polytechnic University

This project is submitted in partial fulfillment of the requirements for the degree of bachelor of engineering in electrical engineering.

Palestine Polytechnic University
Hebron – Palestine

June - 2010

Palestine Polytechnic University
Hebron – Palestine

# Design a single channel EEG system and processing the corresponding signals using HMM

**By**

Hamza F. Altakroury

Shehdeh A.M. Zahdeh

According to the direction of the project supervisor and by the agreement form the entire committee's members. This project was submitted to department of electrical engineering in College of Engineering and Technology to partially fulfill of the B.Sc requirements.

Department Administrator Signature

Name: _____

Project Supervisor Signature

Name: _____

June - 2010

# الإهداء

إلى رمز الحنان إلى الشمعة التي لا تنطفئ إلى رفيقة دربي
أمي الغالية...

إلى الأغلى والأعز على القلب من بين العباد إلى رمز العطاء
إلى أبي العزيز...

إلى كل من تحرك القلم في يده يخط كلمة خير تشرق بها شموس الفجر

إلى إخواني وأخواتي وزملائي وإلى كل من علمني حرفاً

إلى شهداء الوطن الحبيب الذين امتزجت دمائهم بثرى الوطن ليرسموا لنا طريق
الحرية

إلى من وهبوا حريتهم لينيروا طريق العز والشموخ
إلى أسرانا الأبطال

وإلى كل من ساهم في إنجاح المشروع

Acknowledgment

To our supervisors Dr. Hashem Tamimi and Eng. Ali Amro for their guidance, support and encouragement. And for all who help us in this project.

## Abstract

**Design a single channel EEG system and processing the corresponding signals using HMM**

**By**

Hamza F. Altakroury

Shehdeh A.M. Zahdeh

**Palestine Polytechnic University – 2010**

**Supervisor**
**Dr. Hashem Tamimi**
**Eng. Ali Amro**

The idea of Brian Computer interface solves the problems of the disables by analyzing their brain signals. These signals are acquired in the form of Electroencephalogram signals and then processed by the computer which controls other devices.

This project aims to design a hardware device that is able to acquire the brain signals related to Motor Imagination with minimal noise effects. Then these signals are analyzed using Discrete Hidden Markov Model with the help of Fuzzy C-means Clustering and Discrete Cosine Transform.

The results show that we were able to distinguish between silence state, left and right movements with high acceptable response time and low error rate. These results urge us to build a system in the Simulink to perform a real-time processing.

يقوم هذا المشروع على مبدأ مساعدة الأشخاص المصابين بإعاقات حركية من خلال إلتقاط إشارات الدماغ وإدخالها على الحاسوب لتحليلها وفهمها.

كان الهدف في هذا المشروع هو تصميم جهاز متكامل يقوم بإلتقاط إشارات الدماغ ومعالجة هذه الإشارة قبل إدخالها إلى الحاسوب، الذي يقوم فيما بعد بتحليل الإشارة وفهمها. وقد تم التركيز في هذا المشروع على إشارة حركة الأرجل بحيث تم التمييز بين إشارة حركة الرجل اليمين من اليسار من حالة عدم الحركة بنسبة خطأ مقبولة.

# Contents

# List of Figures

# Chapter 1

# INTRODUCTION

## 1.1 Overview

Brain Computer Interface (BCI) is the technology that allows the computer to interact with the brain. This interaction is realized by having computer signals entered into the brain, or by acquiring the signals from the brain to be analyzed using the computer. Fig 1.1 shows the BCI block diagram.

The idea of having external signals penetrate into brain is found in the Neuroprosthetics field, but instead of a full computer, a hardware device is attached to the human skull to help disables to compensate their partially damaged senses.

BCI improves the signal action between human brains and computers in a way that helps the persons who have totally damaged senses to compensate these senses, a good example of that, is the blind man Jens Neumann a man blinded in adulthood became able to drive slowly around the parking area of the research institute [26].

Interacting with the brain could be also based on analyzing signals coming out from the brain. Understanding brain signals means two things; first it is possible to check the healthiness of the brain through these signals, in other words, illness caused due to problems in brain could be recovered. Moreover, BCI is used to understand the imagination of a person. One type of imagination signals is called the *Motor Imagination*, that is the imagination of

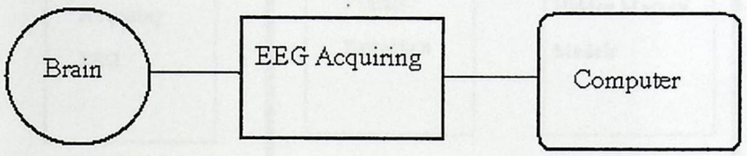


Figure 1.1: BCI block diagram.

body movements.

Motor Imagination helps the disables to compensate their disability or loss in organs, like the loss of hands or legs. Even deaf persons would be understood through BCI.

BCI depends on analyzing the brain signals, these signals are called Electroencephalogram signals, EEG for short, but these signals can not be understood unless a well-designed signal processing technique is established.

## 1.2 Objective

This project tends to design a device which could acquires EEG signals with minimal noise effects. The device is designed to be portable in a way to be easy for the patients to hold it everywhere and every time. Also the project aims to find a reliable signal processing method from which leg movement signals can be understood.

Fig 1.2 summarizes the project in three main stages: The first stage the electronic hardware that aims to acquire the EEG signals. This device is simplified to be only one channel device.
The second stage is the Feature Extraction that aims to find the most significant part of the signal in order to make the job of Hidden Makov Model

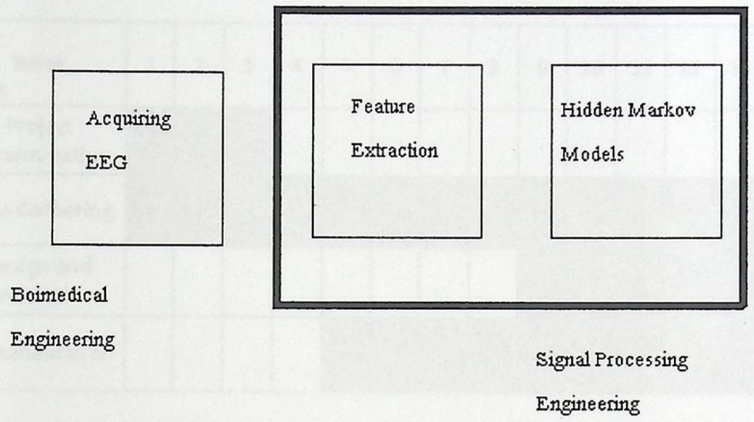


Figure 1.2: Block diagram summurize the project

more efficient and fast.
The final stage is the Hidden Markov Models block, this is a statistical model aims to study random signals like EEG. This block could contain many Hidden Markov Models, where each model is designed to understand only one signal.

## 1.3 Time Schedule

The time plan views the stages in studying, designing and building the entire system. This section includes two time schedules; the first one is done in the first semester while the second shows the task scheduling for the second semester.
Fig 1.3 shows the first semester tasks; all tasks are referred to the theoretical background and the whole system analysis.

Fig 1.4 shows the second semester tasks schedule; all tasks are referred to the implementation and syatem testing.

| Week / Task | 1 | 2 | 3 | 4 | 5 | 6 | 7 | 8 | 9 | 10 | 11 | 12 | 13 | 14 | 15 | 16 |
|---|---|---|---|---|---|---|---|---|---|---|---|---|---|---|---|---|
| Project Determination | | | | | | | | | | | | | | | | |
| Data Gathering | | | | | | | | | | | | | | | | |
| Design and Analysis | | | | | | | | | | | | | | | | |
| Documentation | | | | | | | | | | | | | | | | |

Figure 1.3: Time planning for the first semester

| Week / Task | 1 | 2 | 3 | 4 | 5 | 6 | 7 | 8 | 9 | 10 | 11 | 12 | 13 | 14 | 15 | 16 |
|---|---|---|---|---|---|---|---|---|---|---|---|---|---|---|---|---|
| Hardware Design | | | | | | | | | | | | | | | | |
| Software Design | | | | | | | | | | | | | | | | |
| Implementation and Testing | | | | | | | | | | | | | | | | |
| Documentation | | | | | | | | | | | | | | | | |

Figure 1.4: Time planning for second semester

## 1.4 Economical Study

This section lists the overall cost of the project, these costs are summarize in Fig 1.5.

| Component | Price |
|---|---|
| Printed Board | 100 $ |
| IC's | 50$ |
| Resisters and Capacitors | 20$ |
| Cover and Battery | 30$ |
| Electrodes | 40$ |
| Leads | 100$ |
| Total | 340$ |

Figure 1.5: Hardware Cost

## 1.5 Project Contents

In summary this project contains the following chapters:

- **Chapter 2**: This chapter talks about the physiology of the brain, sources of EEG activity and brain rhythms, it also talks about the electrodes types and their placements.
- **Chapter 3**: This chapter talks about the Hidden Markov Model as a statistical model used in analyzing random signals, this method prove its success in understanding random voice signals.
- **Chapter 4**: This chapter talks about Feature Extraction methods used to get the most important data form the signal therefore easing the manipulation of signals. This method contains both Discrete Fourier Transform and Fuzzy C-means Clustering.
- **Chapter 5**: This chapter describes the design of the EEG device and its electronic components requirements.
- **Chapter 6**: This chapter presents the results of the Signal Processing results tested by MATLAB.
- **Chapter 7**: This chapter explains the implementation of the entier system.
- **Chapter 8**: The final chapter offers a recommendations for those who interest in working in this field.

# Chapter 2

# BACKGROUND

## 2.1 Introduction

In order to analyze an EEG signal some background knowledge about the physiology of the brain (with respect to its biopotentials), and an understanding of what is an EEG signal is necessary. This chapter gives a basic idea about the EEG signals, EEG electrodes placement, and types of EEG electrodes.

## 2.2 The EEG signal

Electroencephalogram (EEG): is a recording of electrical activity originating from the brain. It is recorded on the surface of the scalp using electrodes,

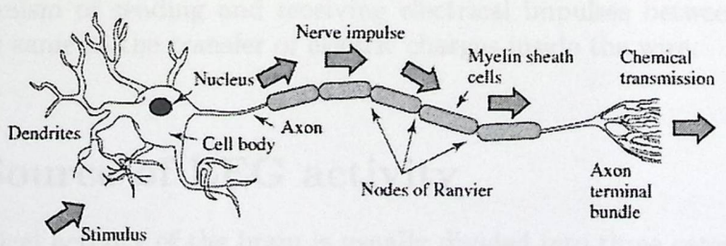


Figure 2.1: The Neuron [2].

# Chapter 2

# BACKGROUND

## 2.1 Introduction

In order to analyze an EEG signal some background knowledge about the physiology of the brain (with respect to its function in muscle control and coordination. standing of what is an EEG signal is necessary). Also a basic idea about the EEG signals, EEG electrodes placement and the electrodes.

## 2.2 The EEG signal

Electroencephalogram (sometimes with thousands) of nerve fibers by different organs and tissues of the body and vice versa. The from the brain neurons that make it contacts together very similar to electrical circuits ,which comes to life when they pass through electricity .Therefore, the mechanism of sending and receiving electrical impulses between nerve cells is the same as the transfer of electric charges inside the wire.

## 2.3 Source of EEG activity

The electrical activity of the brain is usually divided into three categories:

thus the signal is retrievable non-invasively. The brain consists of billions of neurons making up a large complex neural network. Fig 2.1 depicts the Neuron, it has several components: the soma is the cell body of the neuron and contains the nucleus, which houses genetic information; the dendrites extend from the soma, and receive chemical messages from other neurons; the axon transmits electro-chemical signals to other neurons; the myelin sheath consists of fatty tissue cells that insulate the electrical current flowing through the axon [1, 2].

The brain is "defined as a large soft mass of nerve tissue contained within the cranium, the encephalon". Three major structures compose the brain [4], as shown Fig 2.2:

1. The brain stem-automatic vital system control.

2. The cerebellum-involuntary muscle control and coordination.

3. The cerebrum-voluntary movement, sensation, and intelligence.

The brain also includes tens of billions of brain neurons, these neurons are linked to one large group (sometimes with thousands) of nerve fibers by neighboring synapses, this group transports information (meta nerve) from the brain to different organs and tissues of the body and vice versa. The networks of neurons that make it contacts together very similar to electrical circuits ,which comes to life when they pass through electricity .Therefore, the mechanism of sending and receiving electrical impulses between nerve cells is the same as the transfer of electric charges inside the wire.

## 2.3 Source of EEG activity

The electrical activity of the brain is usually divided into three categories:

thus the signal is retrievable non-invasively. The brain consists of billions of neurons making up a large complex neural network. Fig 2.1 depicts the Neuron, it has several components: the soma is the cell body of the neuron and contains the nucleus, which houses genetic information; the dendrites extend from the soma, and receive chemical messages from other neurons; the axon transmits electro-chemical signals to other neurons; the myelin sheath consists of fatty tissue cells that insulate the electrical current flowing through the axon [1, 2].

The brain is "defined as a large soft mass of nerve tissue contained within the cranium, the encephalon". Three major structures compose the brain [4], as shown Fig 2.2:

1. The brain stem-automatic vital system control.

2. The cerebellum-involuntary muscle control and coordination.

3. The cerebrum-voluntary movement, sensation, and intelligence.

The brain also includes tens of billions of brain neurons, these neurons are linked to one large group (sometimes with thousands) of nerve fibers by neighboring synapses, this group transports information (meta nerve) from the brain to different organs and tissues of the body and vice versa. The networks of neurons that make it contacts together very similar to electrical circuits ,which comes to life when they pass through electricity .Therefore, the mechanism of sending and receiving electrical impulses between nerve cells is the same as the transfer of electric charges inside the wire.

## 2.3 Source of EEG activity

The electrical activity of the brain is usually divided into three categories:

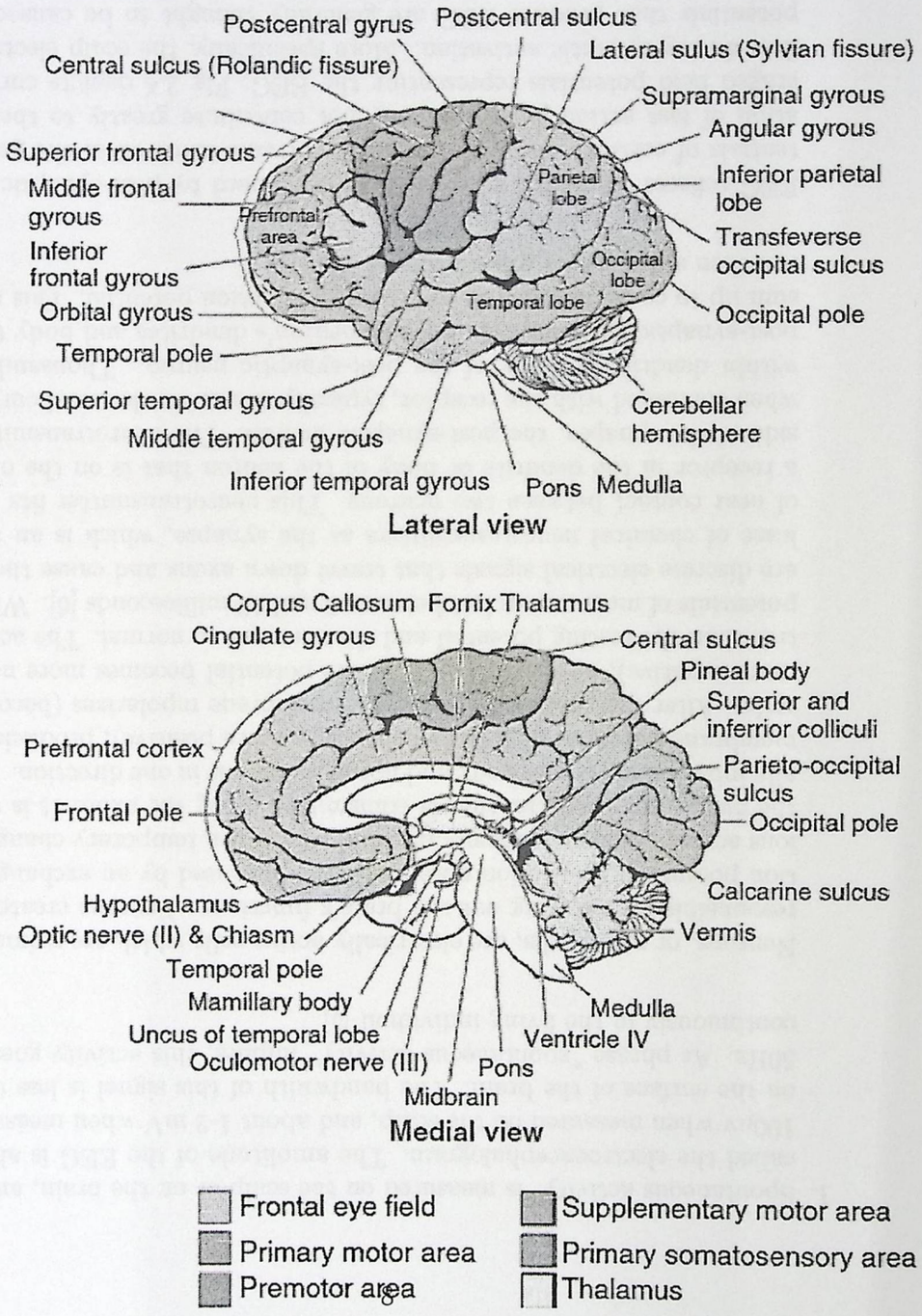


Figure 2.2: The brain and its components.[3].

1. Spontaneous activity: is measured on the scalp or on the brain, and is called the electroencephalogram. The amplitude of the EEG is about 100$\mu$v when measured on the scalp, and about 1-2 mV when measured on the surface of the brain. The bandwidth of this signal is less than 50Hz. As phrase "spontaneous activity" implies, this activity goes on continuously in the living individual [5].

   Neurons, or nerve cells, are electrically active cells which are primarily responsible for carrying out the brain's functions. Neurons create action potentials [3]. Action potential (AP) is caused by an exchange of ions across the neuron membrane, and an AP is a temporary change in the membrane potential that is transmitted along the axon. It is usually initiated in the cell body and normally travels in one direction. The membrane potential depolarizes (becomes more positive), producing a spike. After the peak of the spike the membrane repolarizes (becomes more negative), as shown Fig 2.3. The potential becomes more negative than the resting potential and then returns to normal. The action potentials of most nerves last between 5 and 10 milliseconds [6]. Which are discrete electrical signals that travel down axons and cause the release of chemical neurotransmitters at the synapse, which is an area of near contact between two neurons. This neurotransmitter fits into a receptor in the dendrite or body of the neuron that is on the other side of the synapse, the post-synaptic neuron. The neurotransmitter, when combined with the receptor, typically causes an electrical current within dendrite or body of the post-synaptic neuron. Thousands of post-synaptic currents from a single neuron's dendrites and body then sum up to cause the neuron to generate an action potential. This neuron then synapses on other neurons [3].

   EEG reflects correlated synaptic activity caused by post-synaptic potentials of cortical neurons. The ionic currents involved in the generation of fast action potentials may not contribute greatly to the averaged field potentials representing the EEG; Fig 2.4 depicts current flow during synaptic activation. More specifically, the scalp electrical potentials that produce EEG are generally thought to be caused by the extra-cellular ionic currents caused by dendritic electrical activity, whereas the fields producing magneto encephalographic signals are as-

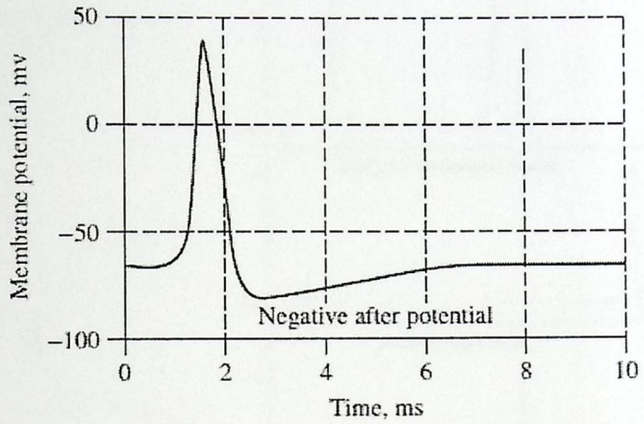


Figure 2.3: An example of Action Potential [3].

sociated with intracellular ionic currents [6].

2. Evoked potentials: components of the EEG that arise in response to a stimulus (which may be electric, auditory, visual, etc.). Such signal are usually below the noise level are not readily distinguished. Hence, and one must use a train of stimuli and signal averaging to improve the signal to noise ratio [5].

3. Bioelectric events produced by single neurons: single neuron behavior can be examined through the use of microelectrodes which impale the cells of interest. Through studies of cell networks actual tissue properties are reflected [5].

   The electric potentials, generated by single neurons, are far too small to be picked by EEG. EEG activity, therefore, always reflects the summation of the synchronous activity of thousands or millions of neurons that have similar spatial orientation, radial to the scalp. Currents that are tangential to the scalp are not picked up by the EEG. Thus, the EEG benefits from the parallel, radial arrangement of apical dendrites

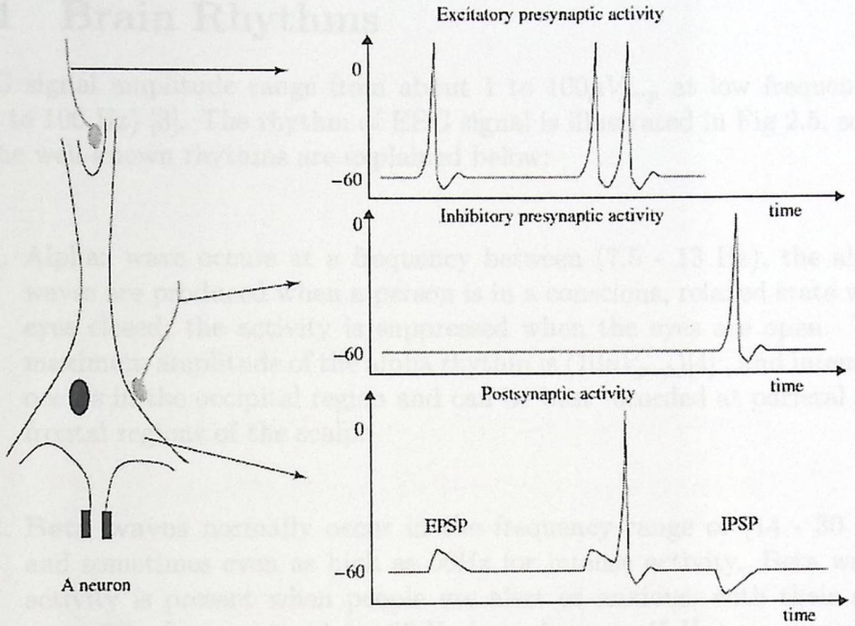


Figure 2.4: The neuron membrane potential changes [5]

in the cortex. Because voltage fields fall off with the fourth power of the radius, activity from deep sources is more difficult to detect than currents near the skull [6].

Scalp EEG activity shows oscillations at a variety of frequencies. Several of these oscillations have characteristic frequency ranges, spatial distributions and are associated with different states of brain functioning (e.g., the various sleep stages). These oscillations represent synchronized activity over a network of neurons. The neuronal networks underlying some of these oscillations are understood, while many others are not [6].

## 2.4 Brain Rhythms

EEG signal amplitude range from about 1 to $100\mu V_{p-p}$ at low frequencies (0.5 to 100 Hz) [3]. The rhythm of EEG signal is illustrated in Fig 2.5, some of the well-known rhythms are explained below:

1. Alpha: wave occurs at a frequency between (7.5 - 13 Hz), the alpha waves are produced when a person is in a conscious, relaxed state with eyes closed; the activity is suppressed when the eyes are open. The maximum amplitude of the alpha rhythm is $(10\mu V_{p-p})$[4] , and intensely occurs in the occipital region and can be best recorded at parietal and frontal regions of the scalp.

2. **Beta waves** normally occur in the frequency range of (14 - 30 Hz) and sometimes even as high as 50Hz for intense activity. Beta waves activity is present when people are alert or anxious, with their eyes open. The frequencies above 30 Hz (mainly up to 45 Hz) correspond to the gamma range (sometimes called the fast beta wave). Although the amplitudes of these rhythms are very low (less than $20\mu V_{p-p}$ in Beta wave, and less than $2\mu V_{p-p}$ in gamma wave ) [4] and their occurrence is rare, detection of these rhythms can be used for confirmation of certain brain diseases.

3. **Theta waves** potentials are relatively large amplitude (less than $100\mu V_{p-p}$)[4], and low frequency (3.5 - 7.5 Hz). Theta waves appeared in sleeping situation, small children, and occur mainly in the parietal and temporal region.

4. **Delta waves** relatively have the largest amplitudes $(100\mu V_{p-p})$[4] and the lowest frequency (0.5 - 3.5 Hz). It is normal rhythm for infants less than one year old and in adults in deep sleep. This wave can thus occur solely within the cortex, independent of the activities in lower regions of the brain [7].

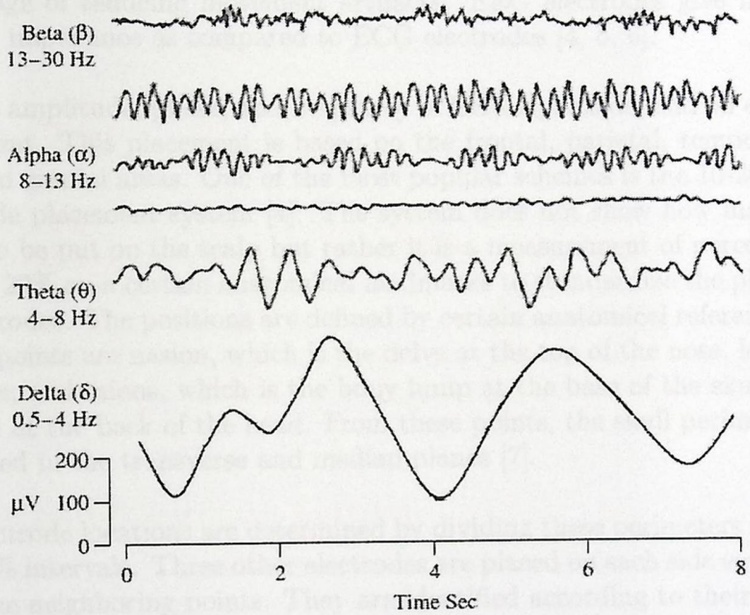


Figure 2.5: Four typical dominant brain normal rhythms [3].

## 2.5 EEG electrodes placement system

The electrical characteristics are determined primarily by the type of metal used. Several types of electrodes can be used to record EEG (Appendix A). EEG electrodes are smaller in size than ECG electrodes. They may be applied separately to the scalp or may be mounted in special bands, which can be placed on the patient's head. In either case, electrode jelly or paste is used to improve the electrical contact. If the electrodes are intended to be used under the skin of the scalp, needle electrodes are used. They offer the advantage of reducing movement artifacts. EEG electrodes give high skin contact impedance as compared to ECG electrodes [4, 5, 6].

The amplitude, phase, and frequency of EEG signals depend on electrode placement. This placement is based on the frontal, parietal, temporal, and occipital cranial areas. One of the most popular schemes is the 10-20% EEG electrode placement system [4]. The system does not show how many electrode to be put on the scalp but rather it is a measurement of percentage of 10% or 20% on a certain anatomical landmarks to standardize the placement of electrodes. The positions are defined by certain anatomical reference. Reference points are nasion, which is the delve at the top of the nose, level with the eyes; and inions, which is the bony lump at the base of the skull on the midline at the back of the head. From these points, the skull perimeters are measured in the transverse and median planes [7].

Electrode locations are determined by dividing these perimeters into 10% and 20% intervals. Three other electrodes are placed on each side equidistant from the neighboring points. They are identified according to their position on the head; Fp for frontal-polar. F for frontal, C for central, P for parietal, T for temporal and O for occipital. Odd numbers refer to electrodes on the left side of the head and even numbers represent those on the right while Z denotes midline electrodes. One electrode is labeled is ground and placed at a relatively neutral site on the head, usually the midline forehead [5].

In addition to the 21 electrodes of the international 10-20% system, intermediate 10% electrode positions are also used. The locations and nomenclature of these electrodes are standardized by the American Electroencephalographic Society. In this recommendation, four electrodes have different names compared to the 10-20% system; these are $T_7$, $T_8$, $P_7$, and $P_8$. These elec-

trodes are drawn black with white text in Fig 2.6. Besides the international 10-20% system, many other electrode systems exist for recording electric potentials on the scalp [5].

Unipolar or Bipolar electrodes can be used in the EEG measurement. In the first method, EEG may be recorded by picking up the voltage difference between an active electrode on the scalp with respect to a reference electrode on the ear lobe or any other part of the body. However, bipolar recording is more popular wherein the voltage difference between two scalp electrodes is recorded; the following Fig 2.7 depicts the Unipolar and Bipolar measurements. Such recordings are done with multi-channel electroencephalographs [5].

Fig 2.8 depicts the position of three electrodes which will be used in this project. Electrode (1) and electrode (2) will be used to acquire the EEG signal using unipolar (Monopolar) method, Monopolar recording is used in research, because it enables the researcher to localize the event of interest. These two electrode fixed in a distance of 5cm in an anterior posterior position on the vertex (Cz according to the international 10-20 system), while electrode (3) is the reference electrode, these positions have been chosen according to the nerves that control the leg motion [8].

## Tissue and Electrode System

The series resistance capacitance equivalent circuit breaks down at the lower frequencies. Where this model would suggest an impedance going to infinity as the frequency approaches DC. To avoid this problem, convert this series RC circuit to a parallel RC circuit as shown Fig 2.9 that has purely resistive impedance at very low frequencies.

Using the simple model of the electrode electrolyte interface of Fig 2.9, as well as the even simpler model previously developed for the electrical activity of the Brain. This overall equivalent circuit, as shown Fig 2.10.

Although C and $C'$, and $R1'$, R2 and $R2'$ may not be exactly equal (different sites and modes of application on the skin), E should be equal to $E'$ (same type of electrode). Hence V represents the actual difference of ionic

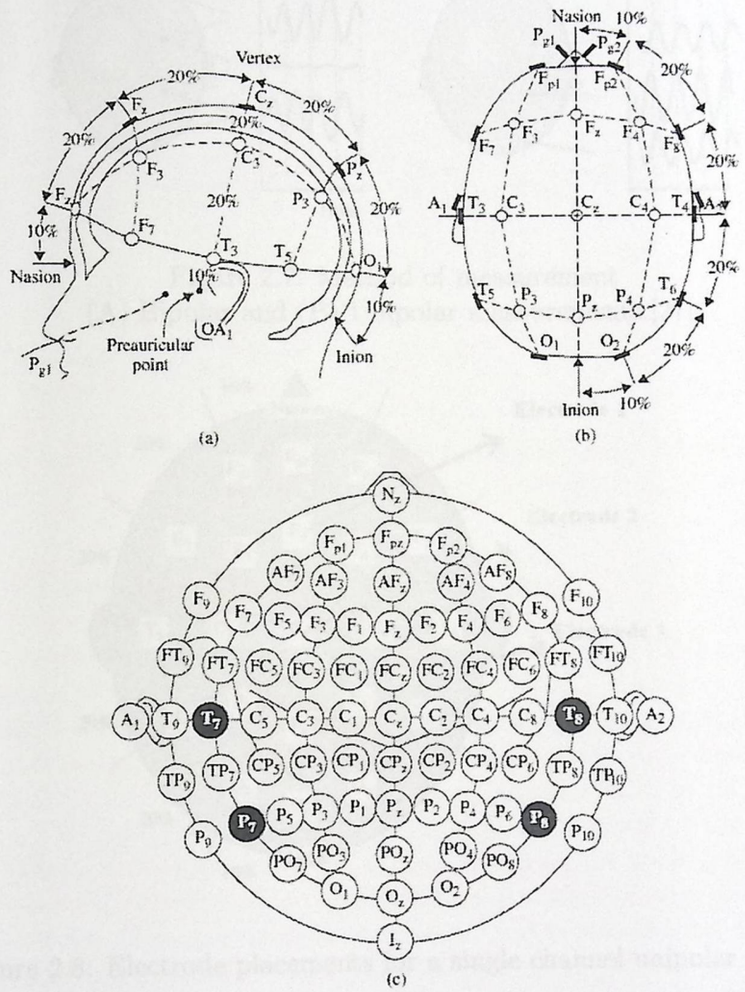


Figure 2.6: The international 10-20% system
seen from (A) left and (B) above the head A = Ear lobe, C = central, $P_g$ = nasopharyngeal, P = parietal, F = frontal, $F_p$ = frontal polar, O = occipital. (C) Location and nomenclature of the intermediate 10% electrodes [3].

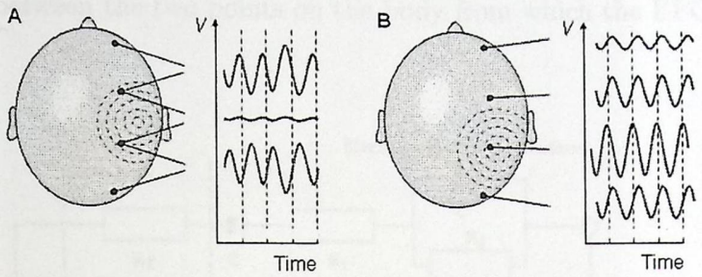


Figure 2.7: Method of measurement
(A) Bipolar and (B) Unipolar measurements.[27].

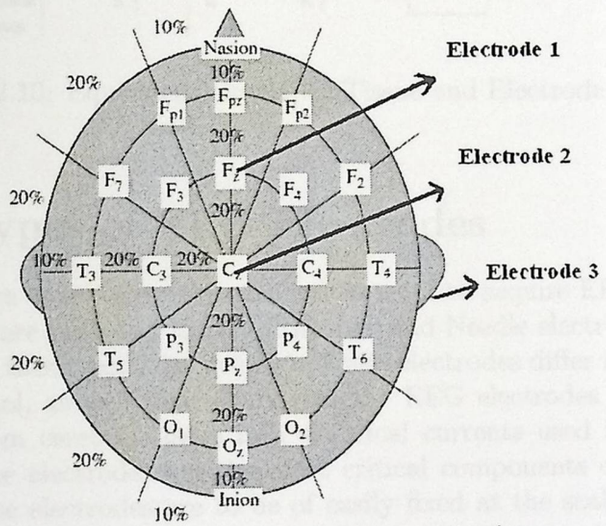


Figure 2.8: Electrode placements for a single channel unipolar system.

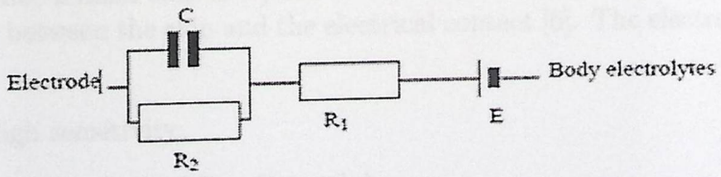


Figure 2.9: Equivalent circuit of the Ag-AgCl Interface[6].

potential between the two points on the body from which the EEG is being recorded.

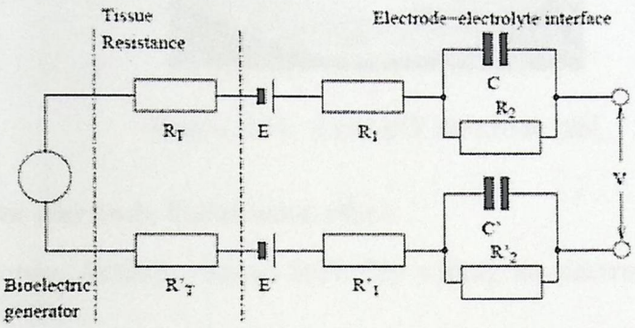


Figure 2.10: Equivalent circuit for Tissue and Electrode system [6].

## 2.6 Types of EEG Electrodes

Several types of surface electrodes can be used to acquire EEG signals. The main types are Suction,Floating, Flexible, and Needle electrodes (Appendix A describes these eectrodes deeply). These electrodes differ in their location in the cranial, as well their configuration. EEG electrodes transform ionic currents from cerebral tissue into electrical currents used in EEG preamplifiers. The electrodes are the most critical components of the recording chain. These electrodes are to be of easily fixed at the scalp with minimal disturbance of coiffure cause no discomforts and remain in place for extended period of time. The disposable self-adhesive pad is selected, we choose this pad because it's noninvasive and ideal for measuring low voltage Brain signals. Since human skin is a poor electrical conductor, a low-resistance gel is applied between the skin and the electrical contact [6]. The electrodes should be:

- High sensitivity.
- Low Electrode Offset Potentials.
- Low Electrode Noise.

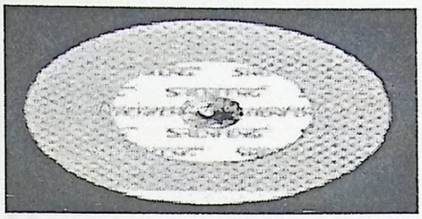

Figure 2.11: Ag/AgCl electrode [28].

- Low Electrode Polarization effect.
- Motion Artifact—about 5mV (By adding an electrode jelly or paste) [5][6][9].

Ag/AgCl electrodes should offer the best combination of low offset potentials and drift, low noise and relative immunity to motion artifact. These disposable electrodes require face to face bench testing to ensure that the offset voltage is less than 100mV, the noise is less than 150$\mu$V the 10Hz impedance is less than 2K, and the bias current tolerance to 200nA for 8 hours yields less than 100mV offset. Hence, Ag/AgCl will be used in this project [3, 8, 10].

# Chapter 3

# HIDDEN MARKOV MODEL

## 3.1 Introduction

This chapter presents the theory of Hidden Markov Model, and how can we utilize it in our project.
Signals are physical quantities produced by variety of real-world processes. These signals can be discrete in nature, such as codebook characters, etc., or continuous in nature such as speech, music, temperature, etc.
All signals are emitted from sources, these sources can be stationary, in which the signal's statistical properties do not vary with time, or nonstationary, in which the signal's statistical properties vary with time.
Signals coming form one source are called pure signals, while those coming form many sources, for example the origin of the signal and the noise source, are called corrupted signals.

Studying real-world signals is achieved using signal models, these models provide the basis for the theoretical description of a signal processing system. Also signal models can be used to process the signal so as to provide a desired output, and they are potentially capable of letting us learn a great deal about the signal source without having to have the source available, i.e. we can simulate the source and learn as much as possible via simulation.

Signal models can be divided into two types, deterministic models and statistical models. Deterministic models exploit some known specific properties of the signal, here the specification of the signal model is generally straight

forward; like estimating frequency, amplitude, etc.In statistical models one tries to find statistical properties of the signal, random processes are used to characterize the signal here.One of the statistical models is called *Hidden Markov Model*, HMM for short, which is going to be applied in this project.

HMM is very common in the field of speech recognition, the theory of HMM was first published in 1960's and first implemented in speech recognition system in 1970's.

## 3.2 Discrete Markov Model

Assume that we have a system with $N$ different states, that is, the system can be in one of its different states at any given time $T$. Let $w_n(t)$ is the $n$ state at time $t$, where $n \in N$, then in the following example:

$$w^T = \{w_1(1), w_4(2), w_3(3), w_2(4)\}$$

the system visit the states 1, 4, 3 then 2, for short, it can be rewritten as:

$$w^T = w_1, w_4, w_3, w_2$$

In general, a full probabilistic description of the systems like the one mention above requires a specification of the current state as well as all its predecessors. So if it is desired to find the probability of any sequence of states, we can use the following formula:

$$P(w_1, w_2, w_3, ..., w_N) = P(w_1) \cdot P(w_2|w_1) \cdot P(w_3|w_1, w_2) \cdot \cdots \cdot P(w_N|w_1, ..., w_{N-1}) \tag{3.1}$$

$$= \prod_{i=1}^{N} P(w_i|w_{i-1}, w_{i-2}, w_{i-3}, \cdots, w_{i-N-1})$$

But in *First Order Markov Process* the probabilistic description depends only on the current state and the previous state, that is:

$$P(w_1, w_2, w_3, ..., w_N) = P(w_1) \cdot P(w_2|w_1) \cdot P(w_3|w_2) \cdot \cdots \cdot P(w_N|w_{N-1}) \tag{3.2}$$

$$= \prod_{i=1}^{N} P(w_i|w_{i-1}, w_{i-2}, w_{i-3}, \cdots, w_{i-N-1})$$

If we define $a_{ij} = P(w_j|w_i)$ which is called the *transition probability* and $\pi_i P(w_i)$ which is the *initial probability*,then the Eq 3.2 becomes

$$P(w_1, w_2, w_3, ..., w_N) = \pi_1 \cdot a_{12} \cdot a_{23} \cdots a_{(N-1)N} \tag{3.3}$$

Usually systems like these are shown graphically as in Fig 3.1

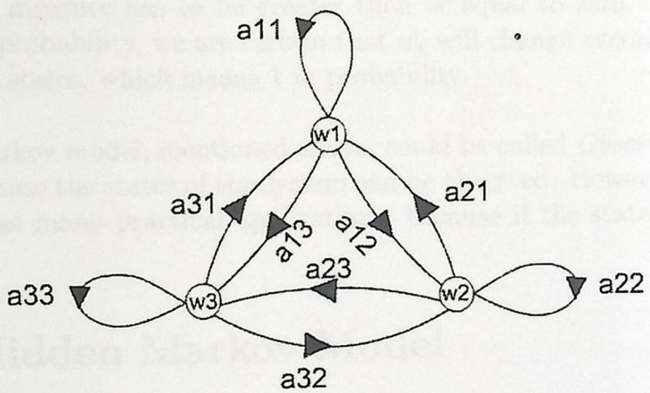


Figure 3.1: Markov Model with three states

The transition probabilities have to obey the standard probabilistic constrains:

$$a_{ij} \geq 0, \tag{3.4}$$

$$\sum_{j=1}^{N} a_{ij} = 1. \tag{3.5}$$

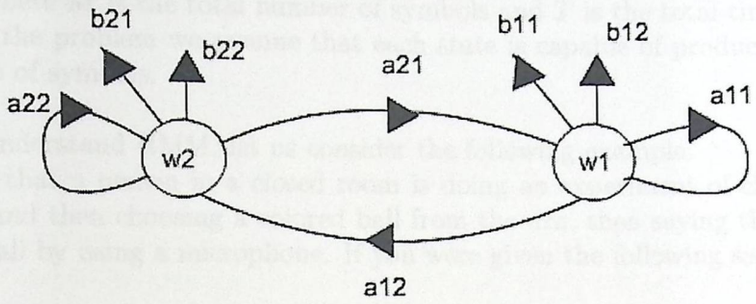


Figure 3.2: Hidden Markov Model with two states and two symbols for each state

Eq 3.4 comes from the basic theorem in probability which states that any probability measure has to be greater than or equal to zero. And Eq 3.5, from basic probability, we are certain that $w_i$ will change *certainly* to one of the defined states, which means 1 in probability.

The Markov model, mentioned above, could be called *Observable Markov Model*, because the states of the system can be observed. However this model does not has many practical applications, because if the states are usually *Hidden*.

## 3.3 Hidden Markov Model

In cases where the source of the signals is not available and/or its states are not observable, Markov Model described previously is not applicable. So it is worth while to use another model, or in other words, a modified model from which the sources and their states can be studied, this model is called the *Hidden Markov Model* HMM.

In HMM, like the one shown in Fig 3.2, it is assumed that any state can be inferred to from an observable symbol assigned to that state, these symbols are, in actual, signals. I.e. Instead of studying the system from its Hidden states, we can study the observable symbols.

The symbols in HMM can be written in the form $v_m(t)$, for $m \in M$ and

$t \in T$, where $M$ is the total number of symbols and $T$ is the total time.
To ease the problem we assume that each state is capable of producing the same set of symbols.

To understand HMM, let us consider the following example:
Assume that a person in a closed room is doing an experiment of choosing an urn and then choosing a colored ball from the urn, then saying the color of the ball by using a microphone. If you were given the following sequence:

$$WYBBBWYYWBYBW...$$

Here the colors of the balls are considered to be the visible symbols, and the urns are the *hidden* states of the model.
The challenge in HMM is choosing the optimal number of unknown states, which is based on the application and can be optimized by find out the output of different experiments.

In general HMM has the following characteristics:

1. The number of states which the system may visit at each time instant. For simplicity we assume that all the states are interconnected, in other words the system is *ergodic*.

2. The number of observation symbols $M$ which is assumed to be constant for the $N$ states, i.e.: each state can emit the given set of symbols.

3. The initial distribution of the system is $\pi_i$, where $1 \leq i \leq N$.

4. The transition probabilities of the system $a_{ij}$, where $1 \leq i, j \leq N$.

5. The emission probability $b_{jk}$, where $1 \leq j \leq N$ and $1 \leq k \leq M$.

The emission probability $b_{jk}$ is defined as following:

$$b_{jk} = P(v_k/w_j) \tag{3.6}$$

$t \in T$, where $M$ is the total number of symbols and $T$ is the total time.
To ease the problem we assume that each state is capable of producing the same set of symbols.

To understand HMM, let us consider the following example:
Assume that a person in a closed room is doing an experiment of choosing an urn and then choosing a colored ball from the urn, then saying the color of the ball by using a microphone. If you were given the following sequence:

$$WYBBBWYYWBYBW...$$

Here the colors of the balls are considered to be the visible symbols, and the urns are the *hidden* states of the model.
The challenge in HMM is choosing the optimal number of unknown states, which is based on the application and can be optimized by find out the output of different experiments.

In general HMM has the following characteristics:

1. The number of states which the system may visit at each time instant. For simplicity we assume that all the states are interconnected, in other words the system is *ergodic*.

2. The number of observation symbols $M$ which is assumed to be constant for the $N$ states, i.e.: each state can emit the given set of symbols.

3. The initial distribution of the system is $\pi_i$, where $1 \leq i \leq N$.

4. The transition probabilities of the system $a_{ij}$, where $1 \leq i, j \leq N$.

5. The emission probability $b_{jk}$, where $1 \leq j \leq N$ and $1 \leq k \leq M$.

The emission probability $b_{jk}$ is defined as following:

$$b_{jk} = P(v_k/w_j) \tag{3.6}$$

As in the case of $a_{ij}$ the emission probability has the properties:

$$a_{ij} \geq 0, \tag{3.7}$$

$$\sum_{k=1}^{M}(b_{jk}) = 1. \tag{3.8}$$

Eq 3.8 states that any state will *certainly* emit one of the defined symbols. Up to now we can conclude that with $b_{jk}$ is doubly embedded stochastic process.

## 3.4 Basic Problems of HMM

HMM has three related problems, these are:

- The Evaluation Problem:
  In this problem, the parameters of the system, $a_{ij}$, $b_{jk}$ and $\pi_i$, are given and the probability of getting a special sequence of symbols $P(v^T)$ is to be determined.

- The Decoding Problem:
  In this problem, the parameters of the models are given, and the optimal path of states $w^T$, that emit the given sequence of symbols $v^T$, is to be found.

- The Learning Problem:
  In this problem initial values of the parameters are given, and it is desired to adjust these values depending on the training sequence of symbols $v^T$.

## 3.5 Computation of Hidden Markov Model

### 3.5.1 Evaluation

The evaluation problem enable us to find the chance of getting a sequence $v^T$ from a specific model, i.e. how likely that $v^T$ can be emitted form the

model.
The evaluation problem is considered as an important problem because, it enables us to choose the best model among set of models, also it helps us to find the likelihood that an unknown signal be generated from the model.

Now we want to find $P(v^T)$, it is given by the equation:

$$P(v^T) = \sum_{r=1}^{r_{max}} P(v^T|w^T) \cdot P(w^T) \tag{3.9}$$

where $r_{max}$ is the total number of combinations given by $N^T$. But $P(v^T|w^T)$ and $P(w^T)$ is given by Eq 3.10 and 3.11.

$$P(v^T|w^T) = \prod_{t=1}^{T} P(v_k(t)|w_j(t)) \tag{3.10}$$

$$P(w^T) = \prod_{t=1}^{T} P(w_j(t)|w_i(t-1)) \tag{3.11}$$

Where $P(v_k(t)|w_j(t))$ is the emission probability and $P(v_k(t)|w_j(t))$ is the transition probability.

Unfortunately this equation needs a huge calculation capacity. To ease the problem estimation we can use the Forward Algorithm or the Backward Algorithm.

### Forward Algorithm

Let $\alpha_i(t)$ be the probability of the system to be in the state $i$ at time $t$ and emit the given symbol $v(t)$. This is simplified in Fig 3.3.

$$\alpha_i(1) = \pi_i \cdot b_{ik}, 1 \leq i \leq N. \tag{3.12}$$

$$\alpha_j(t+1) = \sum_{i=1}^{N} (\alpha_i(t) \cdot a_{ij}) \cdot b_{jk}(t+1), 1 \leq j \leq N. \tag{3.13}$$

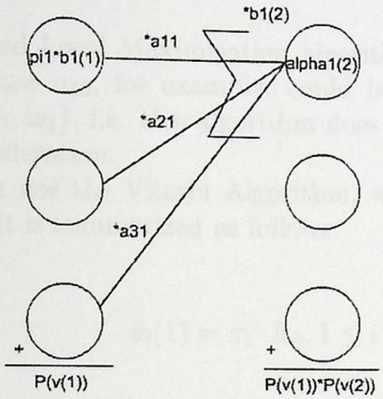


Figure 3.3: Estimating $\alpha$ in Forward Algorithm

$$P(v^T) = \sum_{i=1}^{N} (\alpha_i(T)). \tag{3.14}$$

**Backward Algorithm**

Let $\beta_i(t)$ is the probability of being at state $i$ in time instant $t$, then

$$\beta_i(T) = 1, 1 \leq i \leq N. \tag{3.15}$$

$$\beta_j(t) = \sum_{i=1}^{N} (\beta_i(t+1) \cdot a_{ji}) \cdot b_{jk}(t+1), 1 \leq j \leq N. \tag{3.16}$$

$$P(v^T) = \sum_{i=1}^{N} (\beta_i(1)). \tag{3.17}$$

### 3.5.2 Decoding

Here the parameters and the sequence of symbols are given, in this problem the sequence of the hidden states that generates the given symbols is to be

found. As in the evaluation problem, we find $\alpha_i(t)$ for all $T$ and $N$. Then we consider the maximum value among $N$ in each $t$.

This is called Local Maximization algorithm. But this algorithm is not accurate, because $a_{13}$, for example, could be zero and the maximal path contains $\{..., w_1, w_3\}$, i.e. this algorithm does not take the transition probabilities in consideration.
Instead we can use the Viterbi Algorithm, which is capable of getting the optimal path, it is summarized as follows:
Initialization

$$\theta_i(1) = \pi_i \cdot b_{ik}, 1 \leq i \leq N. \tag{3.18}$$

$$\phi_i(1) = 0. \tag{3.19}$$

Recursion:

$$\theta_j(t) = max_{1 \leq i \leq N}\{\theta_i(t-1) \cdot a_{ij}\} \cdot b_{jk}, 1 \leq j \leq N, 2 \leq t \leq T. \tag{3.20}$$

$$\phi_j(t) = argmax_{1 \leq i \leq N}\{\theta_i(t-1) \cdot a_{ij}\}, 1 \leq j \leq N, 2 \leq t \leq T. \tag{3.21}$$

Termination:

$$p(T) = argmax_{1 \leq i \leq N}(\theta_i(T)) \tag{3.22}$$

$$p(t) = \phi(t+1)(p(t+1)) \tag{3.23}$$

A simple example is shown in Fig 3.4

### 3.5.3 Learning

In the learning problem, which is performed once at the beginning, we try to adapt the model to specific pattern represented by a sample or training sequence. Here the model is trained so that any sequence similar to the training sequence will be generated with high probability.
Our objective here is to adjust $a_{ij}$, $b_{jk}$ and $\pi_i$ for all i and j.

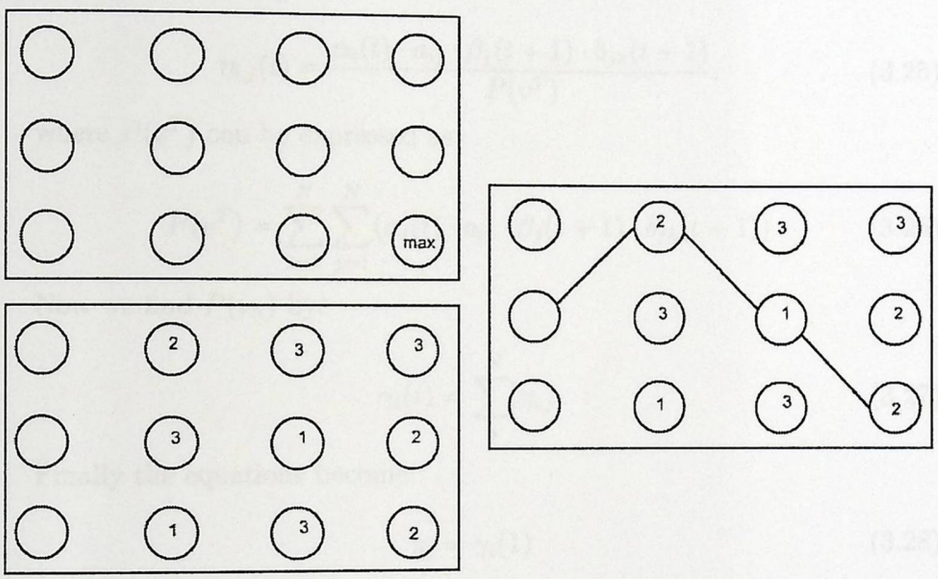


Figure 3.4: Example of Viterbi Algorithm where the upper right image is $\theta$ and lower right is $\phi$, then the optimal path is shown in the right

### Learning Computation

We can define $a_{ij}$ as:

$$\frac{P(w_j, w_i)}{P(w_i)} \tag{3.24}$$

So we want to find $P(w_j, w_i)$, which can be found by the forward-backward algorithm shown in Fig 3.5.

$$\eta_{i,j}(t) = \frac{\alpha_i(t) \cdot a_{ij} \cdot \beta_j(t+1) \cdot b_{jk}(t+1)}{P(v^T)}. \tag{3.25}$$

where $P(v^T)$ can be expressed as:

$$P(v^T) = \sum_{i=1}^{N} \sum_{j=1}^{N} (\alpha_i(t) \cdot a_{ij} \cdot \beta_j(t+1) \cdot b_{jk}(t+1)) \tag{3.26}$$

Now we find $P(w_i)$ by:

$$\gamma_i(t) = \sum_{j}^{N} \eta_{i,j}. \tag{3.27}$$

Finally the equations become:

$$\pi_i = \gamma_i(1) \tag{3.28}$$

$$a_{ij} = \frac{\sum_{t=1}^{T} \eta_{i,j}(t)}{\sum_{t}^{T} \gamma_i(t)} \tag{3.29}$$

$$b_{ij} = \frac{\sum_{t=1}^{T} \delta_i(t)}{\sum_{t}^{T} \gamma_i(t)} \tag{3.30}$$

where $\delta_i(t) = \gamma_i(t) \cdot b_{ik}$.

In the paper publish by Lee and Choi [20] used 2 HMMs for the right hand and 2 HMMs for the left hand, but in their paper they used Continuous HMM instead of Discrete.

This project will use Discrete HMMs, using Discrete Hidden Markov Model simplify the theory and the manipulation and even more logic to

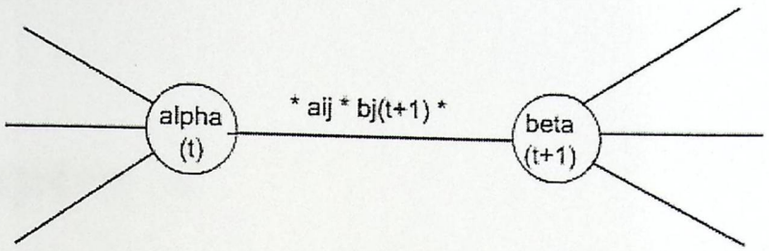


Figure 3.5: Forward-Backward Algorithm

be programmed into programmable devices.

# Chapter 4

# FEATURE EXTRACTION

Hidden Markov Model is very efficient to be aware of the pattern of the signal, but the signal in its original form cannot be entered in the HMM for either training or evaluation.
The signal originally is time varying and may have any value versus time, these values must be known precisely if the signal to be input directly into HMM, because HMM asks about the number of symbols that the signal has. To solve this problem a Feature Extraction methods are used to make the symbols defined in HMM as minimum as possible.

## 4.1 Frequency Domain Representation

The EEG signals are known to have very limited frequency components in their frequency domain. Many references tend to manipulate the first 100 frequency components of the EEG signals [3]. And this is a very attractive property to manipulate the EEG signals in their frequency domain.

Using the frequency components in processing EEG signal make it easy for the system to concentrate on limited frequency components instead of processing the whole signal.

Transforming any signal into its frequency domain is done by using the very popular formula found by the French mathematician Jean Baptiste Joseph Fourier which was named after him [23]. The following equation

is known as the Fourier Transform equation

$$X(f) = \int_{-\infty}^{\infty} x(t) \cdot e^{(-2\pi ft)} dt \tag{4.1}$$

It is also known as the Continuous-Time Fourier Transform because it deals with continuous data.

Most of the applications deal with discrete data because they used computers to process their signal. Computers deal only with discrete data, so instead of using the above equation, the following Discrete-Time Fourier Transform must be used:

$$X(f) = \sum_{n=-\infty}^{\infty} x(n) \cdot e^{(-2\pi fn)} \tag{4.2}$$

The output of Fourier Transform is complex data in general, but the theories in this project deals only with real data points. To avoid dealing with complex numbers only real part, imaginary part or the magnitude has to be taken into consideration.

### 4.1.1 Discrete Cosine Transform

The Discrete Cosine Transform is simply the real part of the Discrete-Time Fourier Transform. Taking the real part of Eq 4.2 the following equation will be evolved which is known as the Discrete Cosine Transform:

$$X(f) = \sum_{n=1}^{N} x(n) \cdot \cos(2\pi fn) \tag{4.3}$$

where N is the window length

This equation is used in many applications related to signal and image processing like image compression, and its output is real number data point. In this project Eq 4.3 is used to transform the signal into its frequency domain.

Transforming the signal into its frequency domain reduce the dimensions of the signal, because EEG signals have limited frequency components, but

until now the problem of determining the symbols to be entered into the HMM is not solved. The frequency domain only reduces the dimension of the EEG data signals which are going to be processed, therefore additional theory must be found to help in estimating the number of symbols.

## 4.2 Clustering

Clustering is the operation of assigning a group of data points into subgroups, these subgroups are called clusters. Each cluster is given a label and so its data point related to it. Here instead of dealing with each data point individually, it is possible to deal with a limited and manageable number of groups. Clustering aims to expand the uniqueness of the signal in an efficient way by transforming the pattern of the signal into a sequence of labels, also it can be considered as a tool to reduce the size of the data.

There are many theories that perform the clustering operation. In this project the Fuzzy C-means clustering is used to divide the signal pattern into single label. This label it treated as a single symbol.

### 4.2.1 Fuzzy C-means Clustering

What distinguish the Fuzzy C-means that it assign gradual memberships of the data points in the cluster, instead of assigning the data point completely in one cluster as the Hard C-means theory does. [24]

If the data points are given the following symbols:

$$X = \{x_1, x_2, x_3, ..., x_n\} \tag{4.4}$$

And clusters are:

$$\Gamma_1, \Gamma_2, ..., \Gamma_c \tag{4.5}$$

Then it is possible to define the degree of membership as $U$, where $u_{ij}$ is a degree of membership of the $j$ data point into the $i$ cluster. The degree of membership is given a values between 0 and 1, where zero degree of membership means no membership, and 1 means full membership.

Two constrains must be under consideration when studying Fuzzy C-means. The first states that there must be no empty cluster, this is clarified by the following equation:

$$\sum_{j=1}^{n} u_{ij} > 0, \qquad \forall i \in \{1, ..., c\} \tag{4.6}$$

The another constrain states that each datum receives the same weight in comparison to all the other data, this appears in the following equation:

$$\sum_{i=1}^{c} u_{ij} = 1, \qquad \forall j \in \{1, ..., n\} \tag{4.7}$$

The algorithm of the Fuzzy C-means depends on the Objective Function, this function is defined as following:

$$J_f(X, U, C) = \sum_{i=1}^{c} \sum_{j=1}^{n} u_{ij}^m d_{ij}^2 \tag{4.8}$$

where $d_{ij}$ is the distance between the $i$ center and the $j$ element. $m$ is the weighting exponent and it is usually equal 2 for the Fuzzy C-means Clustering.

Note that the distance is used as a parameter of similarity between the data and the cluster also note that the membership is inversely proportional with the distance.
It is easy to be aware that the best result of clustering occurs when the highest value of membership $u_{ij}$ encounter the smallest value of distance $d_{ij}$ so the objective is to minimize the squared distance of data points to their cluster centers and so get the maximum degree of memberships.

The algorithm that is used to get the best result of Fuzzy C-means Clustering is called the Alternating Optimization (AO) Scheme, the is $u_{ij}$ are optimized for fixed cluster centers, then the cluster centers are optimized for fixed memberships as the equations clarify

$$U_\tau = J_U(C_{\tau-1}) \tag{4.9}$$

$$C_\tau = J_C(U_\tau) \tag{4.10}$$

The $J_C$ and $J_U$ are obtained by deriving the Objective Function $J_f$ and make it equal to zero. By doing so the following equation evolved:

$$u_{ij} = \frac{d_{ij}^{\frac{-2}{m-1}}}{\sum_{l=1}^{c} d_{lj}^{\frac{-2}{m-1}}} \tag{4.11}$$

$$c_i = \frac{\sum_{j=1}^{n} u_{ij}^m x_j}{\sum_{j=1}^{n} u_{ij}^m} \tag{4.12}$$

Note in Eq 4.11 that it does not depend only on the distance between the data points and their center but also it depends on the distance between data point and the centers of other clusters.
Initially cluster centers are determined randomly before the first update of the membership equation Eq 4.11.

Fuzzy C-means clustering is used in many publications,like [25] that used the wavelet space to extract the feature of EEG signals then FCM is used to maximize the separability of different signals.

# Chapter 5

# SYSTEM DESIGN

This chapter talks about the design of the overall system and its two major parts; the EEG acquiring system and the design of the signal processing system.

## 5.1 Introduction to Acquiring System Design

The EEG signal like other biopotentials is a relatively small signal that exists in the level of ambient noise. The EEG amplifier shall acquire the small EEG signal, amplify it without any significant distortions, and suppress any noise below a sufficient level. This task can be described by basic requirements.

In order to design an EEG system, an understanding of exactly what is an EEG artifacts is necessary. This chapter consists basically of two sections, the noise artifacts of EEG, and EEG hardware .

## 5.2 EEG Noise and Artifacts

EEG signals may be corrupted by various kinds of noise. The main sources of noise are:

- Power-line interference: 50\60 Hz pickup and harmonics from the power lines.

- Electrode contact noise: variable contact between the electrode and the skin, causing baseline drift.
- Motion artifacts: shifts in the baseline caused by changes in the electrode-skin impedance.
- Muscle contraction: electromyogram-type signals (EMG) are generated and mixed with the EEG signals.
- Respiration, causing drift in the baseline.
- Electromagnetic interference from other electronic devices, with the electrode wires serving as antennas, and noise coupled from other electronic devices, usually at high frequencies. For more details Appendix B describes EEG artifacts.

In summary, the EEG signals - which range from $20\mu V$ to $100\mu V$ - are combined with a differential mode dc component of up to 300mV resulting from the electrode skin contact, plus a common mode component of up to 1.5V resulting from the power line potential between the electrodes and ground.

Generally the common mode noise can be minimized by using EEG amplifier that features high common mode rejection ratio (CMRR), and by applying Notch filter circuit. Whereas the differential mode noise can be minimized by using suitable filters.

The skin electrode impedances may differ by as much as 20k$\Omega$ in magnitude. The EEG source impedance is relatively high. Thus, the input impedance of the amplifier should be much higher than the source impedance to minimize the source impedance effects.

## 5.3 Typiccal Biomedical Measurement Systems

As mentioned before the EEG amplifier shall have high CMRR which is defined as the ratio of differential mode gain over the common mode gain to attenuate the line frequency interference that causes approximately the same

voltage between the amplifier inputs and ground (common mode voltage). Also the input impedance of the amplifier should be high enough to prevent the problems resulting from source impedance unbalances.

Since source impedance unbalances mainly caused by electrodes are not uncommon and sufficient rejection of line frequency interferences requires a minimum CMRR of 100dB, the input impedance of the amplifier should be at least $10^9\Omega$ at line frequency (50Hz) to prevent noise due to source impedance unbalances from deteriorating the overall CMRR of the amplifier.

In order to provide optimum signal quality and adequate voltage level for further signal processing, the amplifier has to compromise between providing high voltage gain and avoiding the desired signal distortion. Also it needs to maintain the best possible signal-to-noise ratio.

## 5.4 Overall System Design

The aim of this section is to design a portable EEG system. Fig 5.1 depicts the main components of the hardware system, the electrodes will be used to transform the ionic current in tissue of brain to electrical current, INA circuit amplify the useful signals, and reduce the common mode voltage by high CMRR, HPF to eliminate the DC offset voltage, Notch filter to remove the residual common mode voltage, inverting amplifier to amplifying the signal, and LPF eliminate the high frequency noise above 80Hz.

### 5.4.1 Electrodes and Cables

The disposable self-adhesive pad selected secures to the patients skin and connects to the electrode. We choose this pad because it was noninvasive and ideal for measuring low voltage brain signals. Since human skin is a poor electrical conductor, a low-resistance gel is applied between the skin and the electrical contact. Ag/AgCl Electrode is chosen (section 2.6 describes why we have chosen this electrode). The patient cable is a shielded cable that carries the electrical signal to the INA, Fig 5.2 show the electrodes and leads that carries the signal to INA.

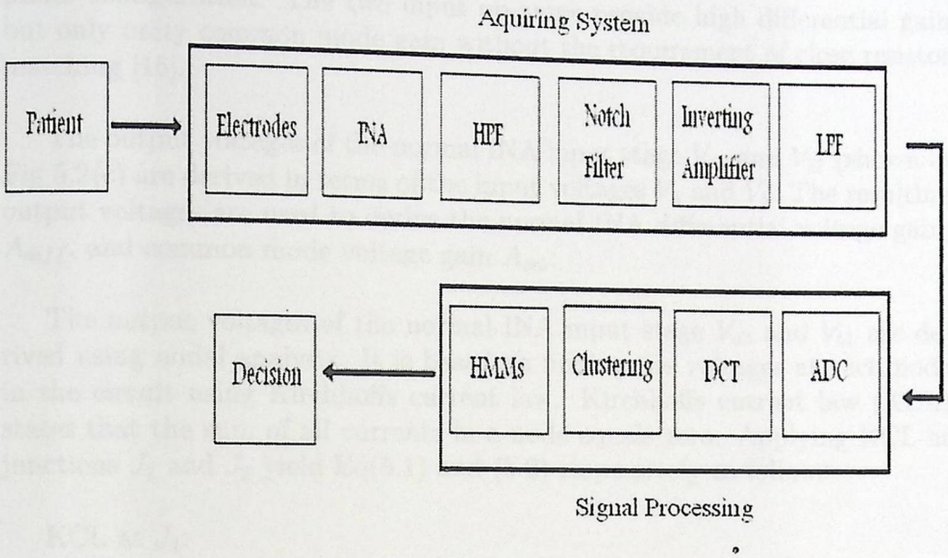


Figure 5.1: Block diagram of EEG system.

### 5.4.2 Instrumentation Amplifier (INA)

The main tasks of the EEG amplifier input stage are to detect the voltage between two electrodes while suppressing the common mode signal and minimizing the effect of EEG source impedance. Thus, such a differential amplifier cannot be realized using a standard single op-amp design (A3 in Fig 5.2), as this doesnt provide the necessary high input impedance. To attain high input impedance, two non inverting amplifiers could be implemented to the input terminals of the single op-amp as shown in Fig 5.2(a). However, the non inverting amplifiers will amplify any common mode voltage. With the same amount as the differential voltage gain, the typical high common mode noise level may drive the amplifier to saturation. Hence the non inverting amplifiers could be replaced by voltage followers, as shown in Fig 5.2(b), which provide high input impedance and unity gain. With the input buffers working at unity gain, all the common mode rejection must be accomplished in the output amplifier, requiring very precise resistor matching. Additionally, the noise of the final op-amp is added at a low signal level, decreasing the signal-to-noise ratio unnecessarily. The circuit in Fig 5.2 (c) eliminates this disadvantage. It represents the normal instrumentation am-

plifier configuration. The two input op-amps provide high differential gain but only unity common mode gain without the requirement of close resistor matching [15].

The output voltages of the normal INA input stage $V_{a1}$ and $V_{b1}$ (shown in Fig 5.2(c) are derived in terms of the input voltages $V_a$ and $V_b$. The resulting output voltages are used to derive the normal INA differential voltage gain, $A_{diff}$, and common mode voltage gain $A_{cm}$.

The output voltages of the normal INA input stage $V_{a1}$ and $V_{b1}$ are derived using nodal analysis. It is based on finding the voltages at each node in the circuit using Kirchhoffs current law. Kirchhoffs current law (KCL) states that the sum of all currents in a node equals zero. Applying KCL at junctions $J_1$ and $J_2$ yield Eq(5.1) and (5.2) respectively as follows

KCL at $J_1$:

$$\frac{V_{a1} - V_a}{R_{f2}} = \frac{V_a - V_b}{R_{g2}}$$

$$V_{a1} = V_a + \frac{R_{f2} \cdot [V_a - V_b]}{R_{g2}} \tag{5.1}$$

KCL at $J_2$:

$$\frac{V_{b1} - V_b}{R_{f2}} = \frac{V_b - V_a}{R_{g2}}$$

$$V_{b1} = V_b + \frac{R_{f2} \cdot [V_b - V_a]}{R_{g2}} \tag{5.2}$$

Subtracting Eq(5.1) from Eq(5.2) yields

$$V_{a1} - V_{b1} = [1 + \frac{2R_{f2}}{R_{g2}}] \cdot [V_a - V_b] \tag{5.3}$$

From Eq(5.3), the normal INA differential voltage gain, $A_{diff}$, can be derived as follows

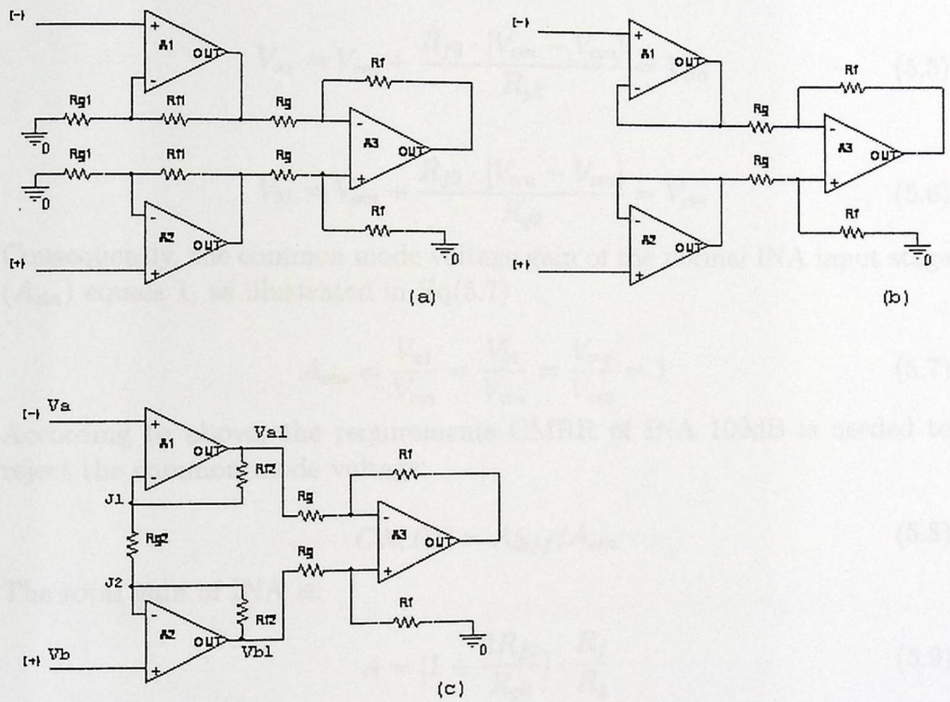


Figure 5.2: Circuit Drawing for Three Different Realizations of INAs Non Inverting Amplifiers input stage (a), Voltage Follower Input Stage (b), and improved, amplifying input stage (c)[15].

$$A_{diff} = 1 + \frac{2R_{f2}}{R_{g2}} \tag{5.4}$$

The common mode voltage gain of the INA input stage $A_{cm}$ can be determined by assuming $V_a = V_b = V_{cm}$, and calculating the corresponding output voltages $V_{a1}$ and $V_{b1}$. Eq(5.1) and (5.2) are written here as Eq(5.5) and (5.6) respectively, with plugging in $V_{cm}$ for $V_a$ and $V_b$

$$V_{a1} = V_{cm} + \frac{R_{f2} \cdot [V_{cm} - V_{cm}]}{R_{g2}} = V_{cm} \tag{5.5}$$

$$V_{b1} = V_{cm} + \frac{R_{f2} \cdot [V_{cm} - V_{cm}]}{R_{g2}} = V_{cm} \tag{5.6}$$

Consequently, the common mode voltage gain of the normal INA input stage ($A_{cm}$) equals 1, as illustrated in Eq(5.7)

$$A_{cm} = \frac{V_{a1}}{V_{cm}} = \frac{V_{b1}}{V_{cm}} = \frac{V_{cm}}{V_{cm}} = 1 \tag{5.7}$$

According to above, the requirements CMRR of INA 100dB is needed to reject the common mode voltage:

$$CMRR = A_{diff}/A_{cm} \tag{5.8}$$

The total gain of INA is:

$$A = [1 + \frac{2R_{f2}}{R_{g2}}] \cdot \frac{R_f}{R_g} \tag{5.9}$$

From above the AD620 INA chosen , because it has the following characteristics:

1. Low internal noise.

2. High common mode rejection ratio (CMRR of 100dB).

3. High input impedance (10M and above).

4. Power supply $\pm 9V$.

5. Low power consumption.

The fig 5.3 expresses an AD620 INA circuit.

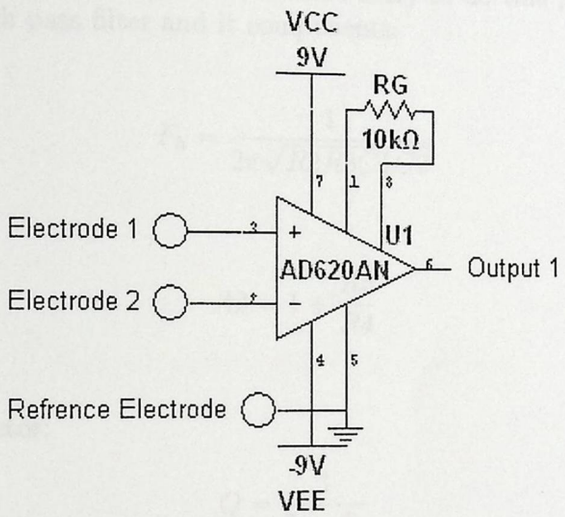


Figure 5.3: AD620 INA schematic.

From the data sheet of this IC, the gain can be calculation by this equation :

$$A1 = \frac{49.9K\Omega}{R_G} + 1 \tag{5.10}$$

Where,

$A_1$ : INA voltage gain.

$R_G$ : External resistance added to achieve a determined voltage gain.

So, the gain that needed in this stage is (6)because the DC offset voltage in milli-volt ,so can't amplifying the signal more than 6 to attenuate the saturation , by using equation (5.10) the value of $R_G$ is 10KΩ.

### 5.4.3 High Pass Filter

After calculating the optimum values of the INA input stage components in previous section , an optimum HPF will be designed in this section to attenuate the slowly varying voltages created by chemical reaction at the electrode patient interface which far exceed the size of the EEG voltages. Higher-order pass filters are required to sharpen a desired filter characteristic, so will be used 2nd order (Sallen-Key Butterworth Filter) to do this purpose. Fig 5.4 depicts the high pass filter and it components.

$$F_h = \frac{1}{2\pi\sqrt{R2R3C1C2}} \tag{5.11}$$

$$A2 = 1 + \frac{R5}{R4} \tag{5.12}$$

Quality Factor:

$$Q = \frac{1}{3 - Av} \tag{5.13}$$

The DC offset frequency that required in this project is Fh =0.5Hz. And the gain not more 3 to avoid accesses to saturation because the residual common mode voltage and ( Q = 0.71) in Butterworth coefficients filter [19],so A =1.5.

Let $C_1$= 330nF , by using equation(5.11):
$R_2$=1MΩ, and $C_1$=$C_2$= 330nF,$R_1$=$R_2$=1MΩ.

The gain of this stage (1.5), so by using equation (5.12), let $R_4$=10KΩ, so $R_5$=5.1KΩ.

The overall gain of these two stages will be:
$A_{total1}$=A1 · A2.
$A_{total1}$= 6 · 1.5

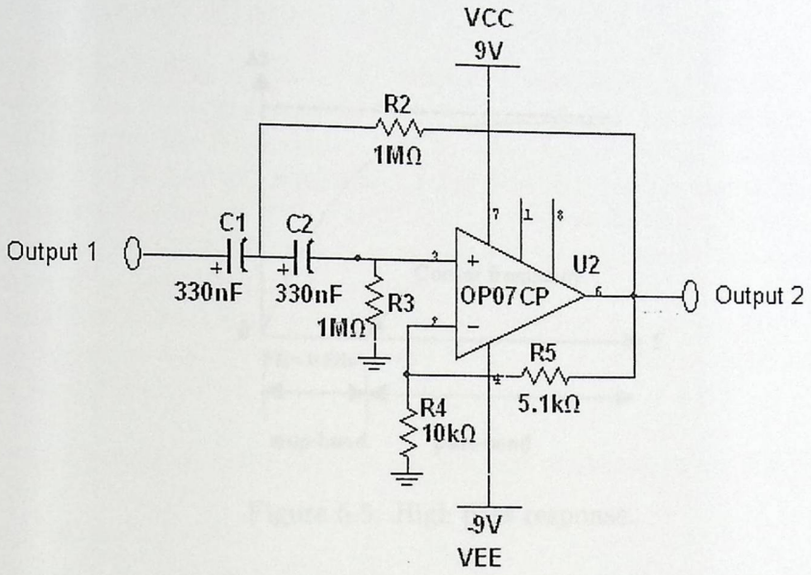


Figure 5.4: 2nd order high pass filter .

$A_{total1} = 9$

Properties of Sallen-Key Filters:

- Simplicity of the design.
- Non-Inverting Amplifier (positive Gain), high input impedance.
- Replication of elements.

The Op-Amps that will be used in this circuit OP07 that has following characteristic:

1. Power supply $\pm 9V$.
2. Low internal noise.
3. Low power consumption.

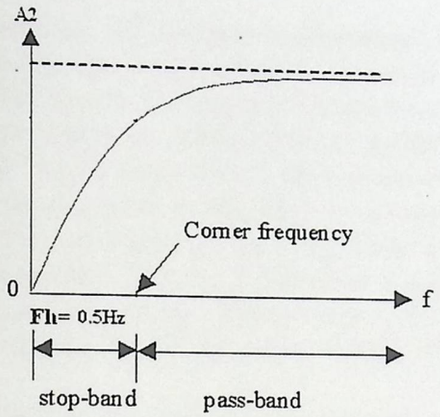


Figure 5.5: High pass response.

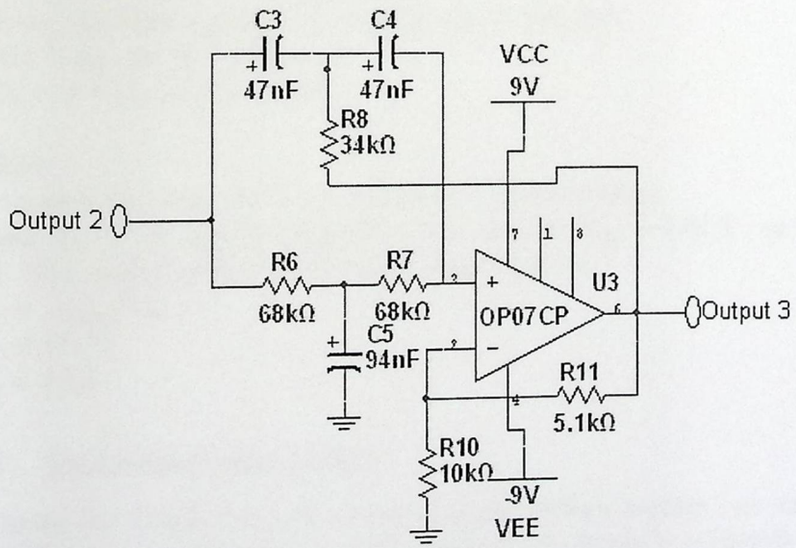


Figure 5.6: Twin-T filter.

### 5.4.4 Notch Filter (50Hz)

From the preceding section, DC voltage is attenuated by the HPF circuit However, the residual common mode voltages created by power line are still combined with the EEG signal. On the other hand, the EEG signals should be amplified to provide adequate voltage level for further signal processing. Hence, the Notch filer will be used. Notch filter is known as band-cut filter or band-reject filter, the function of this filter is to remove some frequency portion of a signal. Fig 5.6 depicts a OP-Amp Twin-T Notch Filter. The Twin-T Notch filter uses one Op-Amp. It based on a passive (RC) that uses three resistors and three capacitors. When deign a Notch filter and band pass filter circuit the Quality factor (Q) must be high [17] [18] .

The formula to calculate the resistor and capacitor values for the notch filter:
$F_{notch} = 1/(2 * \pi * RC)$
$C_3 = C_4 =$ C, and $R_6 = R_7 =$ R.
$F_{notch} = 50Hz$, so by using the previous equation:
Let C = 47nF, So $C_3 = C_4 =$ 47nF.
And From the same equation R=68KΩ, $R_6$=$R_7$=68KΩ.
$R_8 = 0.5 * R_6$ , so $R_8 =$ 34KΩ.
And $C_5 = 2 * C_4$, so $C_5 =$ 94nF.

Where :
$F_{notch}$=center frequency of the notch filter in Hertz (50Hz).
The gain $A_3 = 1.5$, and by using Eq 5.12 , and let $R_{10} =$ 10KΩ , so $R_{11} =$ 5.1KΩ. The overall gain of these three stages will be :
$A_{total2} = A_{total1} * A_3$
$A_{total2} = 9 * 1.5$
$A_{total2} = 13.5.$

### 5.4.5 Inverting Amplifier

After using the Notch filter the common mode voltage remove , so now can be amplified the relatively pure EEG signal as the signal is relatively small in (microvolt). Hence, an inverting amplifier (U4) is implemented to amplify the desired signal ($A_4$ = -50), inverting Amplifier will be used because the bias current is zero and non-inverting terminal is virtual ground. Fig 5.7

depicts the inverting amplifier and its components.

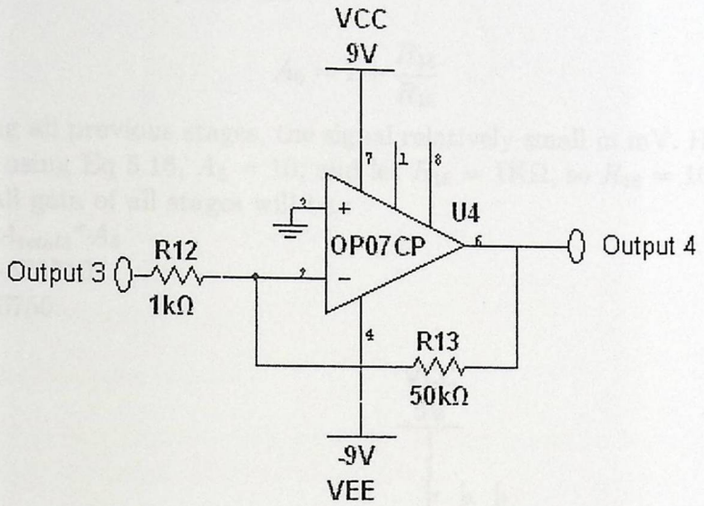


Figure 5.7: Inverting amplifier.

The gain of this amplifier

$$A_4 = -\frac{R_{13}}{R_{12}} \tag{5.14}$$

By using Eq 5.14, $A_4$ = -50, let $R_{12}$ = 1KΩ, so $R_{13}$ = 50KΩ
The overall gain of these four stages will be :
$A_{total3} = A_{total2} * A_4$
$A_{total3}$ = 13.5*-50
$A_{total3}$ = -675.

### 5.4.6 Active Low pass filter

A low-pass filter, as shown Fig 5.8, passes low-frequency signals but attenuates frequencies higher than the cutoff frequency up to 80Hz, as shown fig 5.9. In this stage it's enough to using first order low pass filter .

$$F_L = \frac{1}{2 * \pi * RC} \tag{5.15}$$

The cutoff frequency $F_L = 80Hz$, by using Eq 5.15, let $C_7 = 39$nF, so $R_{15} = 51\text{K}\Omega$ .

The gain of this amplifier is :

$$A_5 = 1 + \frac{R_{16}}{R_{15}} \tag{5.16}$$

After using all previous stages, the signal relatively small in mV. Hence, ($A_5$ = 10),By using Eq 5.16, $A_5 = 10$, and let $R_{15} = 1\text{K}\Omega$, so $R_{16} = 10\text{K}\Omega$.
The overall gain of all stages will be :
$A_{total4} = A_{total3} * A_5$
$A_{total4}$ = -675*10
$A_{total4}$ =-6750.

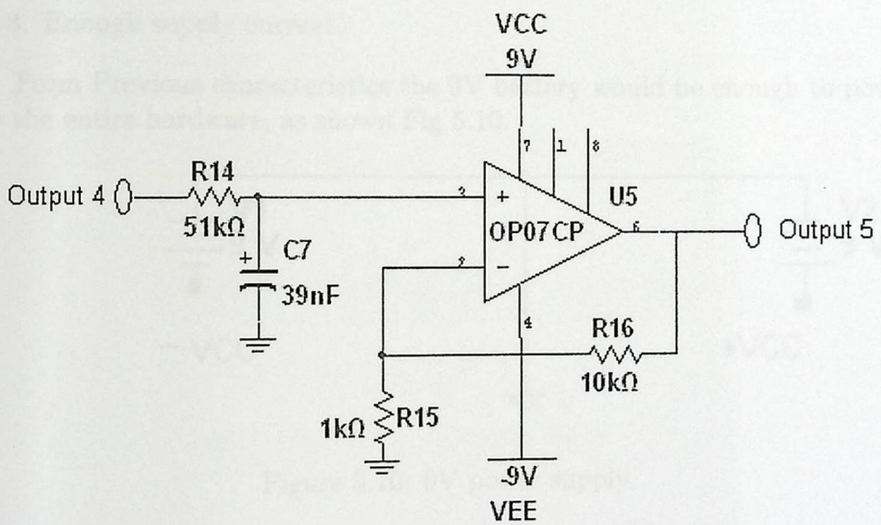


Figure 5.8: Active LPF .

### 5.4.7 Power Supply

The portable device needs power supply to power up the entire hardware , so need a Battery that has the following characteristics:

1. Lightweight.

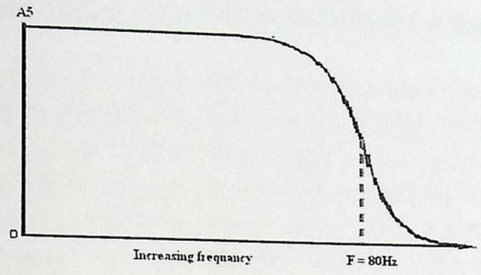


Figure 5.9: Theoretical Response Of LPF .

2. Enough supply voltage.

3. Enough supply current.

From Previous characteristics the 9V battery would be enough to power up the entire hardware, as shown Fig 5.10.

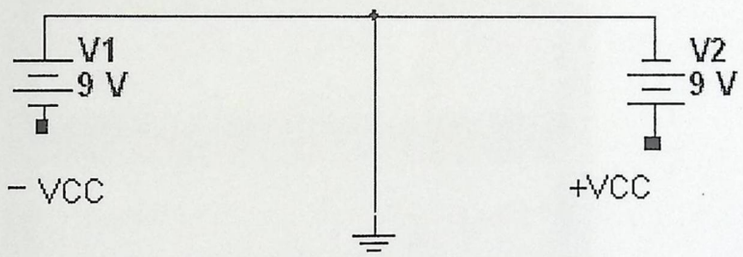


Figure 5.10: 9V power supply.

## 5.5 Introduction to Signal Processing Design

Analyzing EEG signals, in this project, mostly depends on the theory of Hidden Markov Models. Hidden Markov Model, HMM, become familiar with the signals that are used in training the model. The model becomes familiar with such signals by adjusting its parameters according to the input values of the signals during the training phase. And after training the model, it becomes specific for these "training signals" only, now the model can identify and produce such signals.
To make HMM works efficiently, the data on which different HMMs are trained have to be as different as possible. Although the data are generally different the system has to extract this "difference" for HMM. In other words HMM has to deal with parameters of the signals that can be found only in this signals and similar signals.
This project deals with three type of signals; left leg movement, right leg movement and silence state, Fig 5.11.

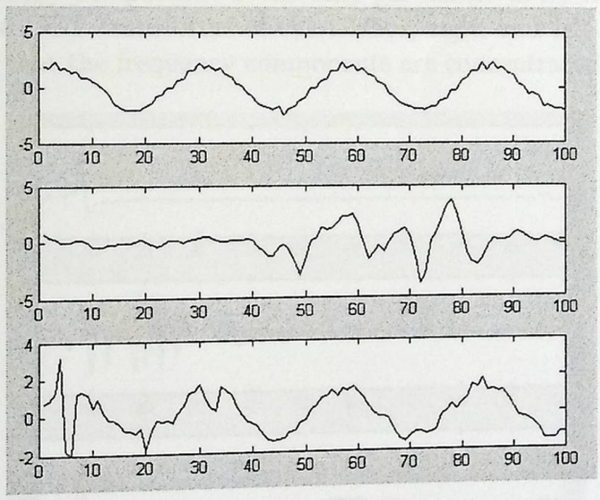


Figure 5.11: Up: silence, middle: right and bottom: left.

## 5.6 Discrete Cosine Transform

Studying signals can be done in time domain or in frequency domain. The signals in time domain can be obtained straight forward from the EEG acquiring system. Processing the signals in time domain has many problems because the amplitude of the signals in time domain is sensitive to noise and it depends on the strength of the movement and the persons that are under the test.
So it is found that the frequency domain can be a solution to the previous problems. On the other hand the frequencies of the EEG signals are limited. Here instead of considering the whole signals it is possible to consider some frequency components between in the interval $[1, 100]$ Hz.

To avoid the effect of the power in the signal, normalizing is used; that is after transforming the signals into its frequency domian it is normalized by dividing its values on the difference between the maximum and minimum. Here the frequency components is the only parameter to be considered. Fig 5.12 shows the DCT transforms of the silence, right and left samples form Fig 5.11, note that the frequency components are concentrated before $30Hz$.

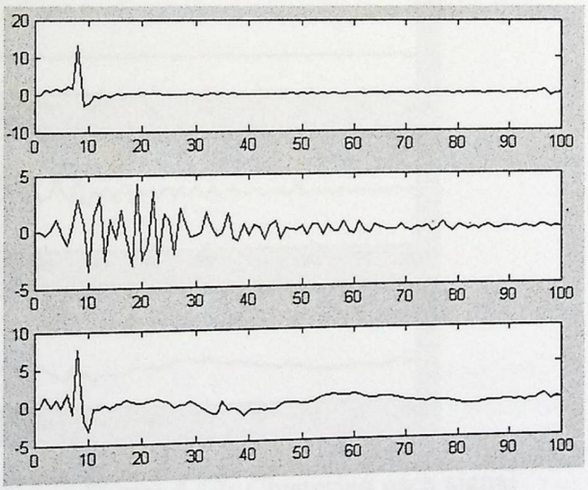


Figure 5.12: DCT of the silence, right and left signals.

## 5.7 Clustering

Transforming the signals into their frequency domain solves only a portion of the problem but not the whole problem. Because entering the data into HMM required the signal to be consists of specific and limited number of symbols, and these symbols have to be defined for the model through the training stage.
To solve this problem it is found that dealing with the amplitude of the frequency components as symbols is not practical because the amplitude of frequency components could vary slightly from signal to another similar signal.

To solve the problem of defining the symbols for HMM, it is estimated that each pattern of the data in the frequency domain can be classified in a specific cluster that has a special label. On other words the pattern of the signal in the time domain can be transformed into a sequence of symbols, each symbol is given according to the form of the potion of the signal, Fig 5.13.

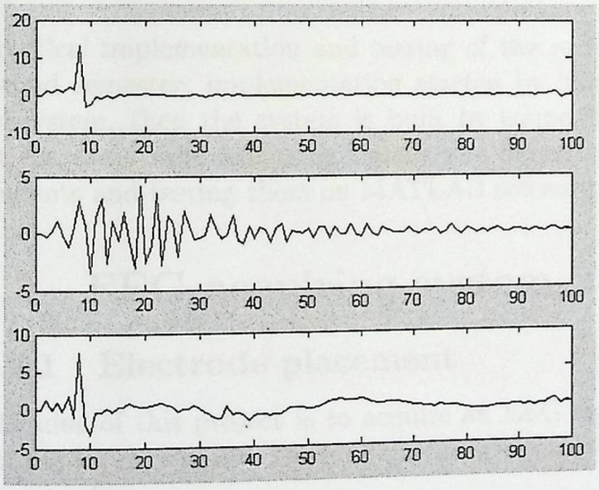


Figure 5.13: Clustering each signal
the window size equal 50 in clustering.

Now with the above constrains are considered, the system is ready to analyze and understand the signals.

# Chapter 6

# IMPLEMENTATION, EXPERIMENTS AND RESULTS

## 6.1 Introduction

Practical implementation and testing of the project have been done in the second semester, implementation started by implementing each individual subsystem, then the system is built by connecting these individual units. At the same time analyzing signals was being done by taking signals form students and testing them on MATLAB software.

## 6.2 EEG acquiring system

### 6.2.1 Electrode placement

The idea of this project is to acquire an EEG signal, which corresponds to patient leg movement. Fig 6.1 depicts the electrode's placement for acquiring the signals.

### 6.2.2 Instrumentation Amplifier (INA)

The INA circuit has been connected as the first component in the project, the following Fig 6.2 views the connection of the AD620 INA, and the result

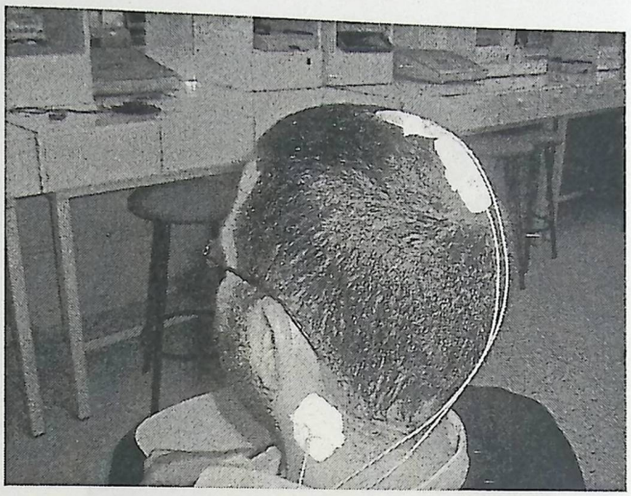

Figure 6.1: Electrodes Placements.

of this stage is shown Fig 6.3.

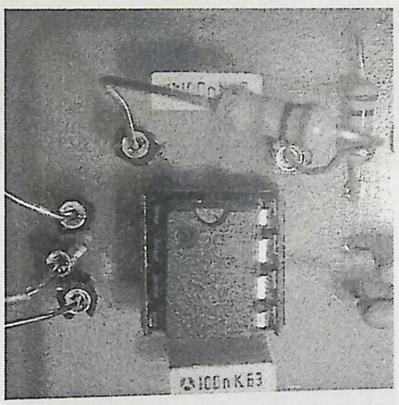

Figure 6.2: AD620 practical connection.

### 6.2.3 High pass filter

This stage show the implementation of 2nd order HPF ,the Opamp that used in this stage is OP07 as shown Fig 6.4, and the result of this stage is shown Fig 6.5.

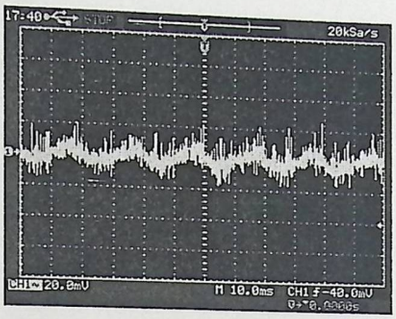


Figure 6.3: Output of INA.

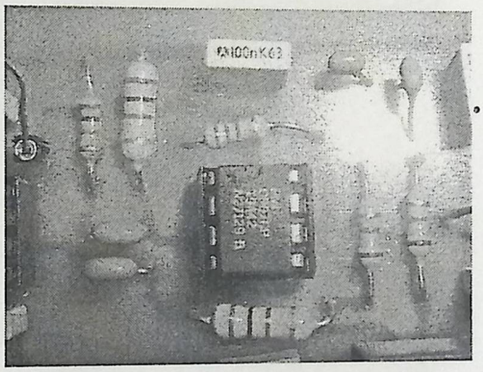


Figure 6.4: 2nd order HPF.

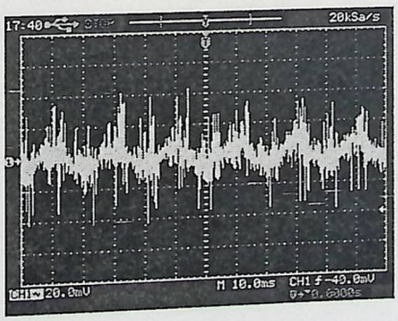


Figure 6.5: Output of HPF.

### 6.2.4 Notch Filter

The Notch filter (shown Fig 6.6) is implemented to remove the residual common mode voltage, Fig 6.7 depicts the result of this stage.

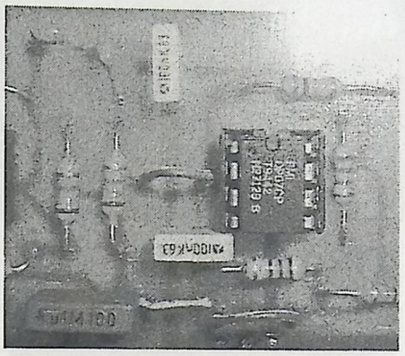

Figure 6.6: Notch Filter.

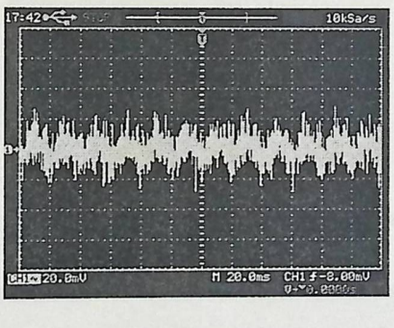


Figure 6.7: Output of Notch filter.

### 6.2.5 Inverting Amplifier

Inverting Amplifier (shown Fig 6.8) is implemented to understand and display the signals by amplifying it, and the result of this stage is shown Fig 6.9.

### 6.2.6 Active Low Pass Filter

LPF is implemented to eliminate the high frequency noise above 80 Hz as shown Fig 6.10, and the result of this stage as shown Fig 6.11.

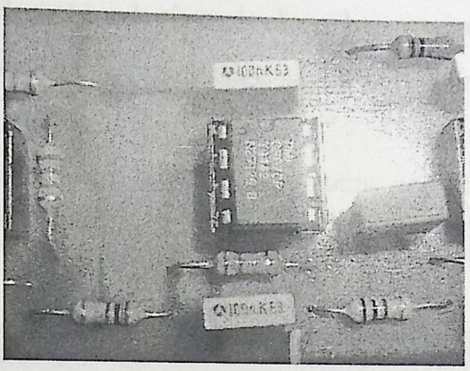

Figure 6.8: Inverting Amplifier.

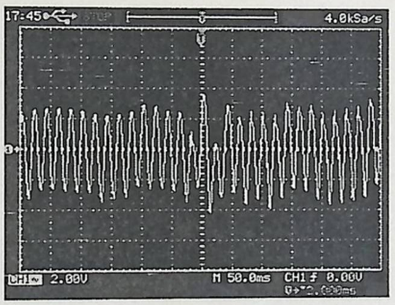


Figure 6.9: Output of Inverting Amplifier.

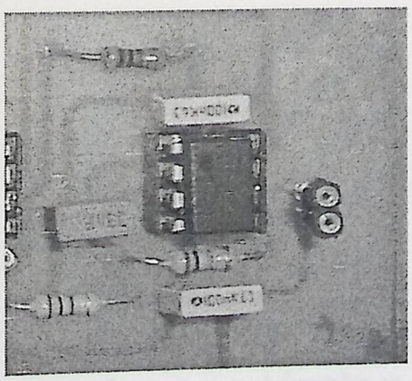

Figure 6.10: Active LPF.

### 6.2.7 Total Practical circuit Implementation

This stage shows all parts of the design and how each connect to other as shown in Fig 6.12.

After implementing all individual subsystems and connecting them together, several output signals of the system are acquired in different cases. The following figures depict the output signals for each state.

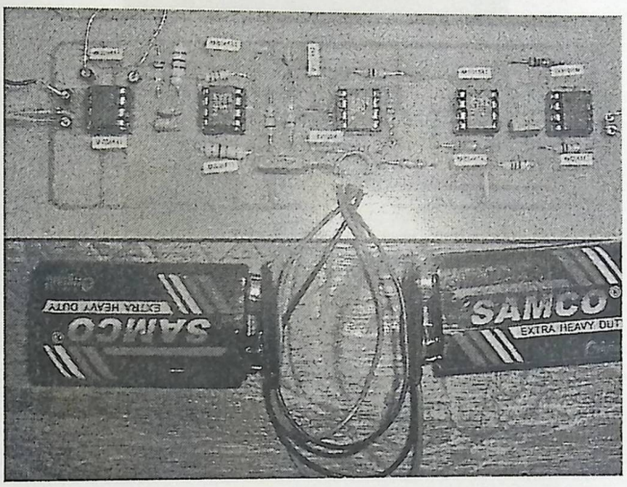


Figure 6.11: Total practical project implementation.

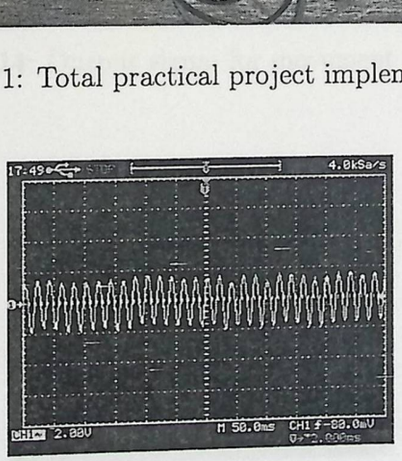


Figure 6.12: Output signal for silence state.

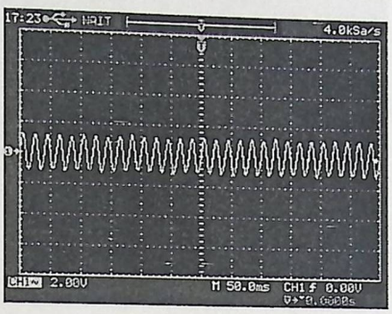


Figure 6.13: silence state with close Eye.

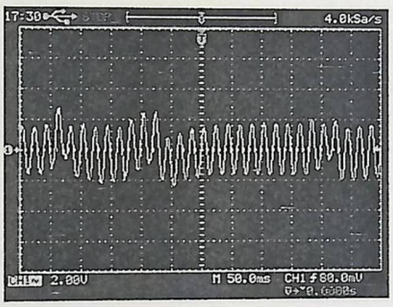


Figure 6.14: Output signal for movement right leg.

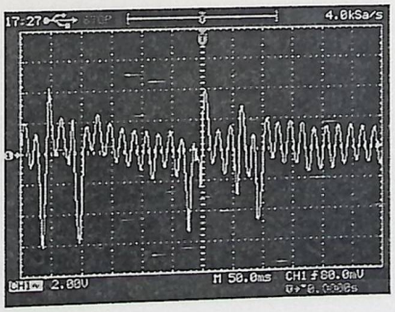


Figure 6.15: Output signal for movement left leg .

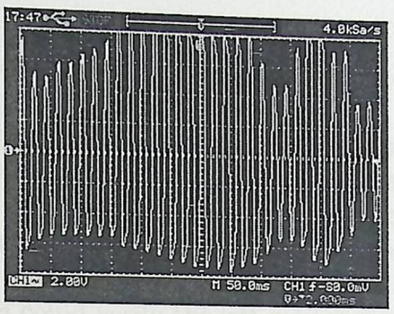


Figure 6.16: Noise from motion around the patient.

## 6.3 Signal Processing Testing

In this project three continuous-movement sets of data are acquired two from the same person at different time and one from a different person. Each set of data contains left movement samples, right movement samples and silence state. In two of the sets the person moved each leg continuously for 98 seconds and the third person moved each for 38 seconds. These data sets are used in what is called three-fold test.

In the three fold test each data set are divided into three portions. Each models are trained on two portion and tested on the third portion. This test is repeated three times because three combinations can be formed from these three portions.
This test is repeated until an acceptable error rate is got with acceptable response time. The parameters of the system that are explained followed are determined through trial and error procedures.
The parameters are found to be:

- The window size 35 sample.
- Frequency components between $[7, 12]$.
- Number of clusters 4.
- Number of states 3.
- Number of symbols in decoding is 5.

These parameters enable the system to identifies the signal with error rates 5% for silence state, 15% for right and 17% for left.

To make sure of the previous results, 5 sets of discontinuous movement are used to verify the results. Two of these 5 sets are acquired from one person and the other three form different three persons. First the models were trained on continuous data and these discontinuous data are used in evaluation stage.
By doing so the system could verify the left movements form the right movements with high precision. But sometimes it is important to change the data on which the models are trained to obtain good results. Of course the silence state is not used because discontinuous data contains silence state.

## 6.4 Steps of training HMM

- Acquiring continuous data.

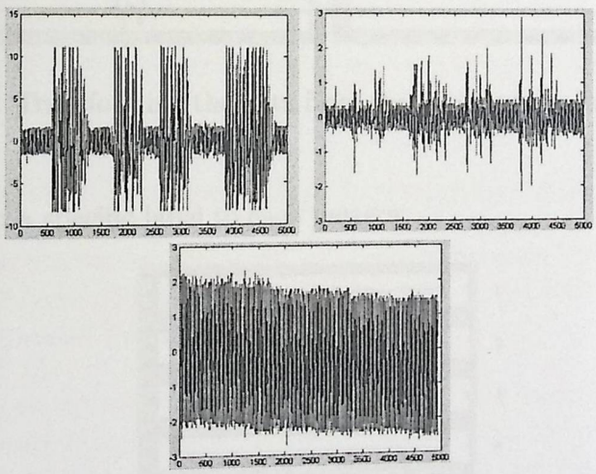

Figure 6.17: Left: data related to the pure left leg movement. Right: data related to the pure right leg movement. Bottom: no motion

- Windowing the data.
- Transforming each window into its frequency domain.

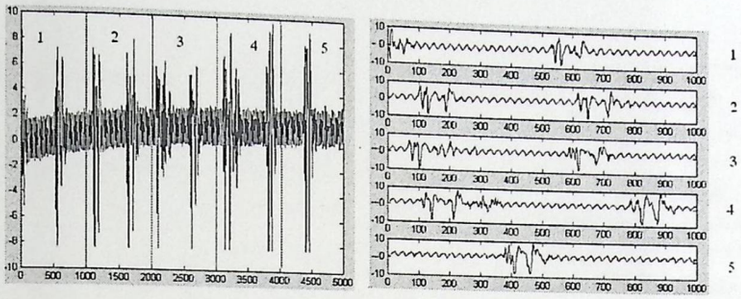

Figure 6.18: Arranging the data in a matrix, here the window size equal 1000

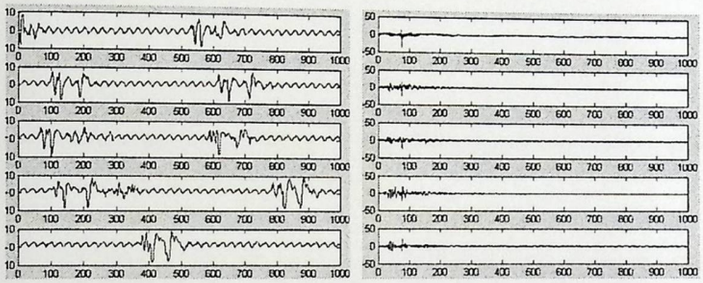

Figure 6.19: Transforming the data from the time domain into the frequency domain

- Assign a specific label to each pattern.

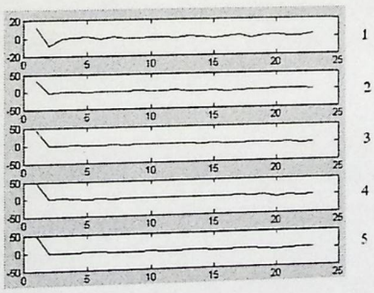

Figure 6.20: Example of labeling the samples, each sample is given a label. Note that two samples may have the same label.

- Training HMM.

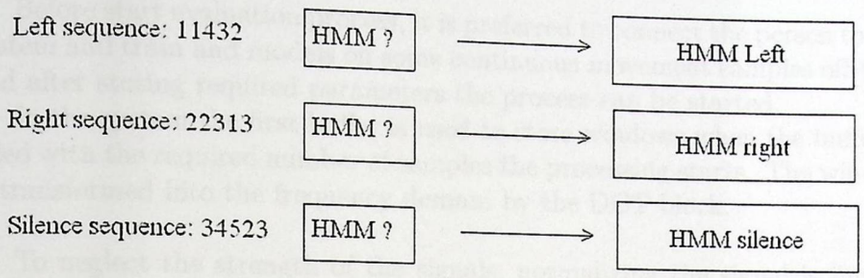


Figure 6.21: Each model is trained on specific sequence of data, after training the model can identify similar signals.

Note that the steps in evaluation are identical with those for training, the difference is that the models in evaluation have the probability measures for specific signals.

## 6.5 Signal Processing Implementation

The implementation of the signal processing hardware is done by using Simulink toolboxes, Simulink enable the system to perform a real-time processing if a suitable acquisition card is used.

This project do not require a complex acquisition card, because the maximum frequency component of the signal equal 30 Hz, by nyquist theorem it is possible to get sample such signal with sampling rate higher than 60 Hz. The DAQ used in this project is the PCI-6024E produced by National Instruments company, it has a 200 kS/sec sample rate and 12 bit resolution. Data sheet for E series DAQ is shown in Appendix D.

In Simulink, the Hardware is implemented using predefined blocks, but some blocks are not found so it was desired to design them in Simulink. After implementing the Hardware in Simulink, the Real-Time Windows Target toolbox is used to obtain real-time processing.

Before start evaluation process, it is preferred to connect the person to the system and train and models on some continuous movement samples off-line, and after storing required parameters the process can be started.

In the system the first buffer is used to store windows when the buffer is filled with the required number of samples the processing starts. The window is transformed into the frequency domain by the DCT block.

To neglect the strength of the signals, normalizing the signal is important, normalizing the signal is done by dividing the signal on the difference between the maximum and minimum.

Distance block performs clustering depending on the stored values, these values represents the center of each cluster. For each window, by now the data buffered in the first buffer is transformed into one symbol.

To get a sequence of symbols the second buffer is required and after the buffer is filled, the sequence of symbols can be entered into HMM. Each HMM is special for one aspect, one for the right leg movement, another for silence state and the third for left leg movement. One thing distinguish one model from another is the predefined probabilities.

The decision maker uses output values of probability to display a specific value, this value represent the kind of movement.

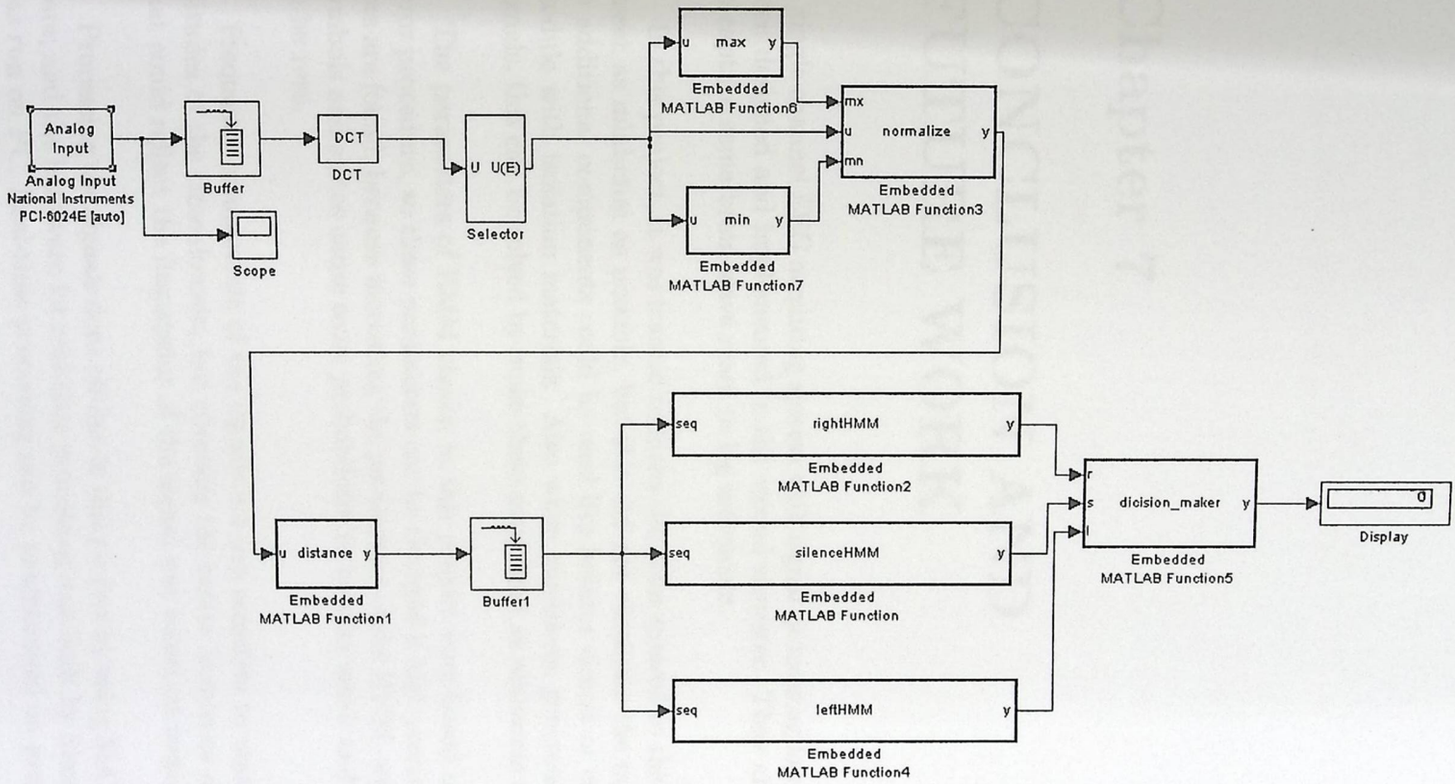


Figure 6.22: Hardware implementation of the system using Simulink

# Chapter 7

# CONCLUSION AND FUTURE WORK

A single channel EEG acquiring system with signal processing hardware have been designed and implemented in the second semester. They are managed to capture some brain wave react to leg movement.

In this project, it was trained to make the noise entered to the signal processer as minimum as possible, but this did not eliminate the noise totally, so additional components could be used like isolator circuit or covering the module with isolation materials. Also wires movement generate unwanted signals, this can be solved by make these movement as minimum as possible.

The parameters of HMM chosen in this project were based on trail and error procedure, so these parameters can be changed if high precision processors are found, because increasing the parameters of the HMM, which are the symbols and states cause some probabilities to be very small and considered to be zero.

Frequency components of the signals are less sensitive to noise than amplitudes of the time domain, but choosing the better frequency components that could reflect the fingerprint of the signal was based on testing.

Processing the signals done off-line in this project by using MATLAB software, and the hardware for real-time processing was built by Simulink which was run on PC. Real-time processing can be programmed on programmable

IC's to make the whole system portable.

# References


[1] R.S. Khandpur , "Hand Book Biomedical Instrumentation " , Center for Electroncs Design and Technology of India , Tata McGraw Hill Publishing Company Limited , 2003 .

[2] Hassanain Ali Lefta Mossa, Electroencephalography EEG, M.Sc. in Medical Engineering from Al-Nahrain University,Iraq 2004.

[3] Saeid Sanei and J.A. Chambers, "EEG SIGNAL PROCESSING",John iley and Sons Ltd, The Atrium, Southern Gate, Chichester, West Sussex PO19 8SQ, England ,2007.

[4] Joseph J.Carr , John M.Brown , Introduction to biomedical equipment technology , Pearson Education ,Fourth Edition ,2003 .

[5] Jaakko Malmivuo, Robert Plonsoy , Bioelectromagnetism ,Oxford New York Toronto, 1995 By Oxford University Press,Inc .

[6] John G.Webster,"Medical Instrumentation", John Wiley and Sons, New York, 1995.

[7] Noor Noorazman, Nor Aziz "Portable EEG Signal Acquisition System" ,College Science in India , 2009 .

[8] S.Ananthi, "A Text Book of Medical Instruments", New AgeInternational(P)Ltd, New Delhi,1st edition 2005.

[9] Colin Binnie,Ray Cooper, Franois manguiere,Jhon Osselton,Pamela Prior and Brain tedman," Clinical Neurophysiology: Eeg, Pediatric Neurophysiology, Special " ELSEVIER SCINCE ,2003.

[10] Gert Pfurtscheller, "EEG-Based Asynchronous BCI Controls Functional Electrical Stimulation in a Tetraplegic Patient",EURASIP Journal on Applied Signal Processing, 31523155, 2005 Hindawi Publishing Corporation, 29 January 2004.

[11] Todd C Handy," Event Related Potential A Methods Handbook", Massachusetts Institute of Technology, 2005.

[12] James N. Knight," SIGNAL FRACTION ANALYSIS AND ARTIFACT REMOVAL IN EEG", Degree of Master of Science Colorado State University, Fort Collins, Colorado, 2003.

[13] Geddes Baker, "Principles of Biomedical Instrumentation", Canada, United States of America, 1989, 3rd edition.

[14] Myer Kutz," Standard Handbook of Biomedical Engineering and Design", The Mcgraw-Hill Compamins, 2003.

[15] Joseph D-Bronzino, "The Biomedical Engineering Handbook" , 2nd edition, volume 1, acid free paper, 2000.

[16] Arthur B.Ritter, Stanley Reisma, Bozena B.Michuiak, "Biomedical Engineering Principles", USA,Acid free pasper, 2005.

[17] - MALVINO, Elctronic Princiles, 6th Edition, The McGraw-Hill Companies, 1999.

[18] Ron Mancini, Op Amps For Everyone, Texas Instruments Incorporated, 2002.

[19] Ainorkhilah Mahmood, zrinawati Mohd Zin, Wan Zarina Wan Kamaruddin and Teoh Sian Hoon, ASSOCIATIO OF HEALTH PROBLEMS WITH 50-HZ MAGNETIC FIELDS IN HUMAN ADULTS LIVING EAR POWER TRAN SMISSION LINES Department of Applied Sciences, Universiti Teknologi MARA Pulau Pinang, Department of Information Technology and Science Quantitative, Universiti Teknologi MARA Pulau Pinang.

[20] Hyekyung Lee and Seungjin Chio, PCA + HMM + SVM FOR EEG PATTERN CLASSIFICATION, Department of Computer Science and Engineering, POSTECH, Koria.

[21] Lawrence R. Rabiner, A TUTORIAL ON HIDDEN MARKOV MODELS AND SELECTED APPLICATION IN SPEECH RECOGNITION, IEEE.

[22] Richard O. Duda, Peter E. Hart and David G. Stork PATTERN CLASSIFICATION 2nd edtion.

[23] Alan V. Oppenheim, Alan S. Willsky and S. Hamid Nawab SIGNAL AND SYSTEMS 2nd edition.

[24] G. Valente de Oliveira and W. Pedryez ADVANCES IN FUZZY CLUSTERING AND ITS APPLICATIONS.

[25] M. Murngappan, M. Rizon, R. Nagarajan and S. Yaacob FCM Clusters of Human Emotions using Wavelet based Features from EEG.

[26] www.wikipedia.org . Last visited: 30 December, 2009

[27] www.bem.fi/book/13/fi/1303.gif.Last visited: 15 Novemper,2009

[28] bioimage.bme.ncku.edu.tw/courses/m05.pdf.Last visited: 20 December, 2009

[29] upload.ecvv.com/upload/Product. Last visited: 20 December, 2009

[30] www.adinstruments.com/products/dataimages/MLA710.jpg. Last visited: 10 November, 2009.

[31] shop.antneuro.com/media/catalog/product/cache/1/image. Last visited: 25 December, 2009

[32] www.neurosigndirect.com/resource/1750.11719.imagelarge.jpg. Last visited: 10 Octobr, 2009

[33] www.namahn.com/resources/documents/note-eyetracking.pdf. Last visited: 29, December, 2009

[34] www.hospimedicaintl.com/images. Last visited: 29 December, 2009

[35] books.google.ps/books. Last visited: 29 December, 2009

[36] www.st-andrews.ac.uk. Last visited: 29 December, 2009

[37] www.linkwitzlab.com/filters. Last visited: 29 November, 2009

[38] www.allaboutcircuits.com. Last visited: 29 December, 2009

[39] www.wikipedia.org . Last visited: 30 December, 2009

# Appendix A

# Electrodes types

## A.1 Suction Electrodes

- No straps or adhesives are required for holding.
- Such electrode are frequently used in ECG as the precordial (chest) leads.
- This electrode can be used only for short periods of time.
- The suction and the pressure of the contact surface against the skin can cause irritation.
- Fig A.1 shows that the actual contacting area is relatively small.
- The electrode is quit large [6].

## A.2 Floating Electrodes

- 5mm curved silver disc-center perforation admits the point of a glass rod by which it can be sealed to the skin until collodion gets dry.

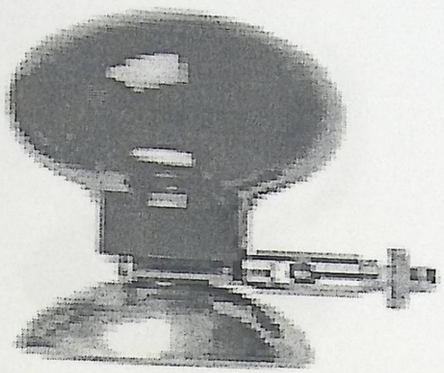

Figure A.1: Suction electrode [32].

- Or it allows spraying through the electrode paste.
- Scarp the skin with needle.
- Useful for restless patients.
- Position cannot be changed [6][8].

## A.3 Flexible Electrodes

- Avoid the curvature that occurs from movement of patient in the body surface.
- Are especially important for monitoring premature infants.

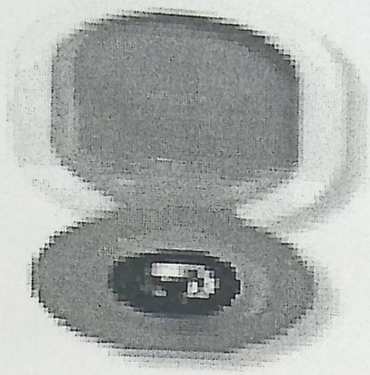

Figure A.2: Adhesive electrode [30].

- They cannot conform to the shape of the infant's chest and can cause severe skin ulceration at pressure points.

- Require some type of adhesive tape to hold them in place against the skin [6].

## A.4 Needle Electrode

- Consists of a solid needle, usually made of Stainless steel or silver, with a sharp point.

- Contact resistance-high.

- A variation of this type of electrode is used on patients undergoing surgery to monitor the EEG continuously [6][8].

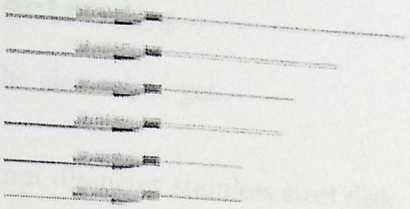

Figure A.3: Needle electrode [31].

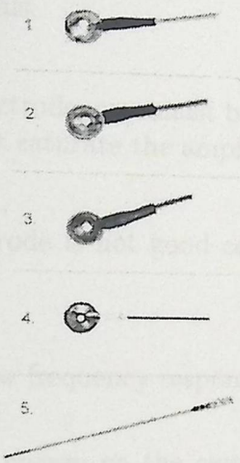


Figure A.4: Sphenoidal Electrodes [32].

## A.5 Sphenoidal Electrodes

- Injection needle 5cm long varnish insulated has a point bare at end.

- Need surgery [6][8].

## A.6 Dry Electrodes

- Not requiring the electrolyte gel.

- Consists of a 7mm diameter stainless steel disk.

- The amplifier that connection with this electrode should locate as close to the electrode as possible to reduce noise from electrostatically detected signals.

- For this electrode, care must be taken that any half-cell potentials that exist do not saturate the amplifier.

- If the electrode is not good contact with the skin, this can have two effects:

    1. The low frequency response of the electrode can be compromised.

    2. If any charge on the capacitance, the changing capacitance can result in a changing voltage and hence artifacts.

- Another serious source of artifacts in this electrode results from the very high impedance amplifier [6] [8].

# Appendix B

# EEG Artifacts

This Appendix discusses different artifacts of EEG and presents methods to remove them.

## B.1 Transient Activities

Artifacts are caused by muscle activity, movement, electrocardiographic (ECG) activity, blood-flow pulse waves, and electrode or equipment problems. Although marked by differences in amplitude, frequency of occurrence, and scalp distribution, share one useful common characteristic for automatized detection of theses artifacts. In particular, they mostly consist of high amplitude spikes that are easily detectable using a peak to peak amplitude test.

### B.1.1 Muscle Activity

Muscle can cause transient high-amplitude spikes, as shown Fig B.1(e), which are mainly generated by scalp and face muscles in frontal and temporal regions; however, they may be recorded by electrodes nearly anywhere on the scalp surface. This type of artifact can often be reduced, or even completely eliminated, by asking the subjects to relax, or change the position. When this type of artifact occurs a single electrode, pushing on or reapplying the electrode can sometimes stop it. These signals have a wide frequency range and can be distributed across different sets of electrodes depending on the

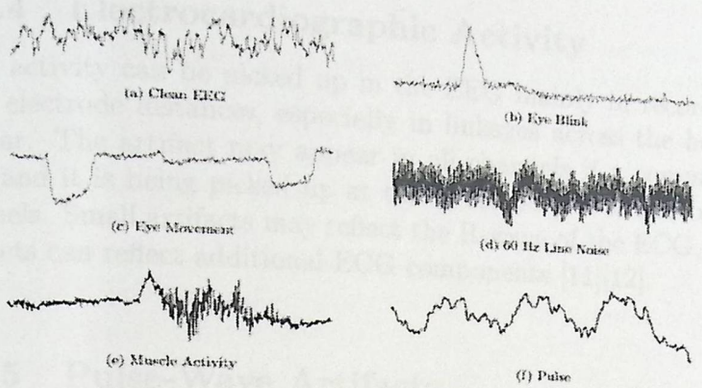


Figure B.1: Artifacts Waveforms .

location of the source muscles [11][12].

### B.1.2 Movement

Head and body movements or movement of electrode wires can cause artifacts even when all electrodes make good mechanical and electrical contact. These types of artifacts are often erratic and not repetitive, unless the movement is rhythmical. This type of artifact can result from tremor, thinking, breathing, or head movements [8][12].

### B.1.3 Movements in the environment

Movement of other persons around the patient can generate artifacts. Another artifact, probably due to electrostatic changes on the drops, can be introduced by a gravity-fed intravenous infusion.

With the increasing use of automatic electric infusion pumps, a new type of artifact, infusion motor artifact (IMA), has arisen. Morphologically, IMA appears as very brief spiky transients, sometimes followed by a slow component of the same polarity. Its frequency does not relate directly to drop rate. This artifact arises from electromagnetic sources.

### B.1.4 Electrocardiographic Activity

ECG activity can be picked up in the EEG mainly in recording with wide inter electrode distances, especially in linkages across the head and to the left ear. The artifact may appear in all channels if a common reference is used and it is being picked up at that reference, or it can be in just a few channels. Small artifacts may reflect the R-wave of the ECG, whereas larger artifacts can reflect additional ECG components [11][12].

### B.1.5 Pulse-Wave Artifacts

The pulse, or heart rate, artifact, as shown Fig B.1 (f), occurs when an electrode is placed on or near a blood vessel. The expansion and contraction of the vessel introduce voltage changes into the recordings. The artifact signal has a frequency 1.2Hz, but can vary with the state of the patient. This artifact can appear as a sharp spike or smooth wave [12].

### B.1.6 Respiration artifacts

Respiration can produce two kinds of artifacts. One type is in the form of slow and rhythmic activity, synchronous with the body movements of respiration and mechanically affecting the impedance of (usually) one electrode. The other type can be slow or sharp waves that occur synchronously with inhalation or exhalation and involve those electrodes on which the patient is lying. Several commercially available devices to monitor respiration can be coupled to the EEG machine. As with the ECG, one channel can be dedicated to respiratory movements [12].

## B.2 Eye Blink Artifact

The eyeball acts as a dipole with a positive pole oriented anteriorly (cornea) and a negative pole oriented posteriorly (retina). When the globe rotates about its axis, as shown Fig B.1(b), it generates a large amplitude alternate current field detectable by any of the electrodes positioned near the

eye. A blink causes the positive pole (the cornea) to move closer to front polar FP1, FP2 electrodes, producing symmetric downward deflections [11][12].

## B.3 Interference Artifacts

From high-frequency radiation from radio, television, hospital paging systems, power lines, and other electronic devices can overload EEG amplifiers. May be introduced either electro statically by unshielded power cables and regardless of current flow, or electromagnetically by strong currents flowing through cables and equipment such as transformers or electro motors. Shielding the offending power cables and cables and using a shielded room for the recording can reduce electromagnetic interference by proper wiring of the power cables. The cutting and/or coagulating electrode used in the operating room also generates high-voltage high-frequency signals that interfere with the recording system. The best thing to do is turn off the EEG machine while using this instrument [13].

### B.3.1 Electrodes-skin Interference

Surface electrodes such as the ones used in EEG must create an interface between an ionic solution (the subject) and a metallic conductor (the electrode). This leads to a half-cell potential which can be quite large relative to the signal being recorded .To minimize this problem of polarization of the electrode, with application of a liquid or gel electrolyte between the skin and electrode. This bridges the electrode surface to the skin. The gel is an aqueous chloride-bearing solution that will hydrate the skin, reduce the impedance of the corneum, and produce a more uniform medium for charge transfer. Skin electrode impedance can drop below 5K$\Omega$across the hydrate skin.Gel electrolyte provides a convenient method of coupling between the silver-silver chloride electrodes to the skin surface. Touching the electrodes during recording can produce artifacts. The most common electrode artifact is the electrode popping, which is due to a sudden change of electrode contact, causing amplitude changes that rise and fall abruptly. The first step in avoiding these types of artifacts is to check all the connections: the electrode may be detached or loose, the lead wire may be broken, or the conductive paste

may have dried. Next, check the electrode impedance. In addition, check that all connections between electrodes and amplifier are sufficiently dry [14].

### B.3.2 Electrical Interference Problems in Bioptential Measurement

Bioelectric potentials are relatively low-level electric signals and must be substantially amplified before a recording can be easily displayed. Modern integrated circuit amplifiers are well suited to this task since they have high gains and contribute little noise to the biopotential measurement [13][14][15].

#### Power Line Interference

In modern society we are immersed in a complex electromagnetic environment originating from power wiring in buildings, radio transmitters of various sorts, radiofrequency-emitting appliances such as computers. And natural sources such as atmospheric electricity. Within the home, environmental electric fields will typically induce in the human body a few tens of millivolts with respect to a ground reference. These fields can be much larger, as high as a few volts, if someone is using a cell phone or is located within a foot of power-line wiring or near a radio station. These induced voltages are thousands of times larger than bioelectric signals from the heart as recorded on the chest surface [14][16][19].

Electric-field coupling between the power lines and the EEG and/or the patient is a result of the electric fields surrounding main power lines and the power cords connecting different pieces of apparatus to electric outlets.

Electric coupling of the body to environmental sources is usually due to proximity capacitance and, to a lesser extent, inductive (magnetic) fields. Capacitive coupling between two objects results from the electric field between them. The space or air gap separating the objects acts as a dielectric. The coupling can be simply modeled as a parallel-plate capacitor, which can be determined by

$$C = \frac{\epsilon \cdot A}{d} \tag{B.1}$$

Where $\epsilon = \epsilon_r \cdot \epsilon_0$, where the individual $\epsilon$ dielectric constants are for free space and air, respectively
$A$ = area of mutual conductor plate interception
$d$ = separation distance

A person usually will have greater coupling to ground than to the power line, perhaps by a factor of 100 or more. As a result, a voltage divider is created, and the body acquires a potential, known as a floating potential $V_{float}$. Its magnitude, as measured by a voltmeter with a ground reference, is determined by the ratio of impedances of the body to the power line $Z_{line}$ ,given in Eq(B.2) , and ground impedance, given in Eq(B.3).

$$Z_{line} = 2\pi f C_{line}. \tag{B.2}$$

$$Z_{ground} = 2\pi f C_{ground}. \tag{B.3}$$

This arrangement is shown in Fig B.2 and ignores any ground resistance since it is usually negligible. The body itself is a volume conductor with such a low relative resistance that it is not significant to this analysis. In this case, a subjects floating potential is given by the impedance divider relationship:

$$V_{float} = \frac{V_{line} \cdots Z_{ground}}{Z_{line} + Z_{ground}} \tag{B.4}$$

The floating potential can be a relatively large induced potential. Take, for example, a person sitting in a metal chair. If the persons proximity capacitance to the power line is assumed to be 1 pF, the ground impedance $Z_{ground}$ is $107\Omega$, and the line voltage is $220V_{rms}$ ($622V_{pp}$) at $50Hz$, then the calculated floating potential is [14].

By using Eq (B.2)and Eq(B.4), the value of $Z_{line}$ was $3.18 * 10^9\Omega$, and $V_{float}$ equal $1.94V_{pp}$.

This $V_{float}$ is present uniformly over the body and will sum with a skin biopotential $V_{bio}$. The output of the amplifier $V_{out}$ is the sum of all potentials at its input. Thus the floating potential is summed with the biopotential:

$$V_{out} = V_{float} + V_{bio} \tag{B.5}$$

In the preceding example, the line induced interference is greater than could be tolerated in a recording. It is an artifact with a sinusoidal waveform characteristic.

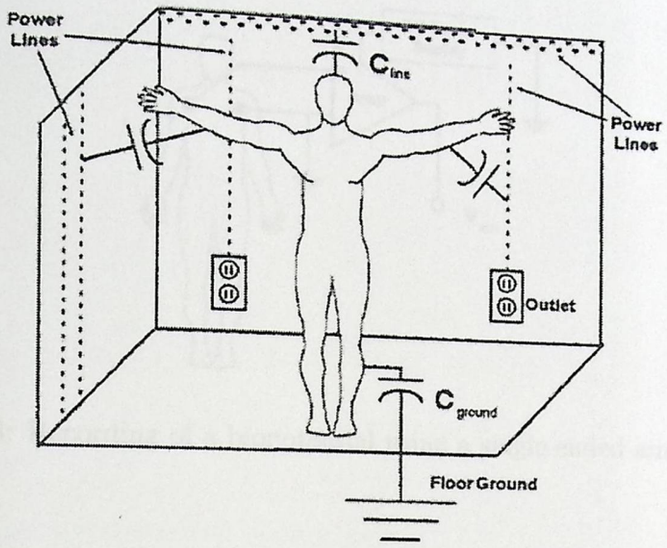


Figure B.2: Illustration of body capacitive line coupling [18].

### Single-Ended Biopotential Amplifiers

A single-ended biopotential amplifier monitors an input voltage with respect to its reference. Its reference completes an electric circuit to the object of study. Because they are simple, single-ended amplifiers, they are sometimes used in biopotential monitoring. They need only two electrodes, a single monitoring electrode and a reference electrode. This kind of amplifier should not to be confused with a differential amplifier, where there are two inputs that subtract from one another. Fig B.3 shows a schematic of a single-ended amplifier where its reference is connected to both the subject and ground [14] [11].

Environmental line-frequency interference coupled to the subject is a major challenge for this amplifier configuration. One approach to reduce interference is to ground the body with a reference electrode to an earth ground. In principle, grounding a biological object will reduce $V_{float}$ to zero if $Z_{ground}$ is zero. With this idealized configuration, a biopotential $V_{bio}$ would be amplified without concern for environmental noise. In practice, bioelectrodes have significant electrical impedances.

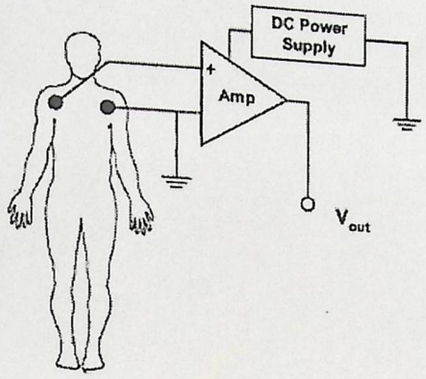


Figure B.3: Recording of a biopotential using a single ended amplifier [18].

This means that the divider ratio defined by $Z_{line}$ and $Z_{ground}$ produces a Vfloat value that is not reduced to zero by the grounding electrode. Therefore, to achieve quality single-ended amplifier recordings, it is essential to minimize coupling capacitance and ensure low-impedance reference electrodes.

Low line-coupling capacitance reduces noise and can often be achieved with small biological specimens by (1) removing the work area from power-wire proximity and/or (2) shielding the specimen with a metal enclosure or copper mesh connected to ground. Capacitive coupling does not occur through grounded conductive enclosures unless line-frequency power wires to equipment are allowed to enter the enclosure.

It is more difficult to shield the human body than biological specimens because of the bodys bulk and greater surface area. Skin-electrode resistance is also greater than that of invasive electrodes used in biological specimens, and this causes higher floating potentials on the human body. Except under certain conditions discussed later, these circumstances can create frustration in using single-ended amplifiers for human recording.

For example, if a subjects electrode-skin impedance $Z_{electrode}$ is 20 k$\Omega$, this value is low enough that it dominates over his or her ground capacitance such that essentially $Z_{ground} = Z_{electrode}$. Assuming the same line-coupling

capacitance as before (1 pF) and using the voltage-divider relation given earlier, the calculated floating potential $V_{float}$ was $3.9mV$ by using Eq(B.4) , it is now much lower , but is greater than could be tolerated in a recording [14][15][16]:

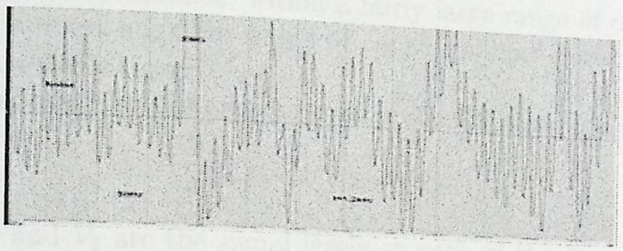

Figure B.4: $50Hz$ Artifacts[32].

### Differential Biopotential Amplifiers

The use of differential amplifiers is common in biopotential measurements because of a greater ability to reject environmental interference compared with ground-referenced single-ended amplifiers. Differential amplifiers subtract the electric potential present at one place on the body from that of another. Both potentials are measured with respect to a third body location that serves as a common point of reference.

Differential amplifiers are useful because biopotentials generated within the body vary over the body surface, but line-coupled noise does not. Environmental electric fields from the power line are more remote and couple such that they are present uniformly over the body. This is partly due to the distributed nature of capacitive coupling. It is also because the low (50-60)Hz line frequencies have electric field wavelengths so long (hundreds of meters) that a persons body can be considered to be, in some sense, an antenna in the uniform near field of an electric field source.

The induced body potential $V_{float}$ is present at both inputs of a difference amplifier, and as used here, it is also known as the common-mode potential $V_{cm}$. This is so because it is common (equal) in amplitude and phase at each of the two amplifier inputs. Thus, for our differential amplifier,

$$V_{cm} = V_{float} \tag{B.6}$$

The connection of a differential amplifier always requires three electrodes since a common reference point for the amplifier is needed. The grounding electrode, as in the preceding single-ended case, also reduces the common-mode potential on the body surface. Even if the ground were not effective due to a large electrode resistance, within a fairly large range of common-mode levels, the differential amplifier would be capable of near-perfect cancellation of the common-mode signal.

Differential amplifiers of gain A perform the following operation:

$$V_{out} = A(V1 - V2) \tag{B.7}$$

Where $V_1$ and $V_2$ are the signal levels on each of the Non-inverting and inverting inputs of the amplifier, respectively, with respect to a reference. In practice, differential amplifiers very closely approach this ideal. Modern differential amplifiers can have common-mode rejection ratios of 120 dB or better, meaning that they perform the subtraction to better than one part per million.

In practice, this interference cancellation process works fairly well; however, the assumption that the power-line-induced signal is common mode (uniform) over the body does not hold perfectly in all situations. Slight differences in its phase or amplitude over the subjects body when in close proximity to some electric field source or unbalanced electrode impedances can cause this cancellation process to be less than perfect. Some line noise may still pass through into the recording. Usually, improvements in skin electrode preparation can remedy this problem [14].

### Frequency Distortion Artifacts

The EEG does not always meet the frequency-response standards that have described in the chapter one. The same EEG when passed through a circuit that has diminished gain at high frequencies, this pattern is said to have high-frequency distortion. And when EEG passed through an amplifier that has inadequate gain for low frequencies, this type is said to have low-frequency distortion [6].

### Saturation or cutoff distortion

High offset voltages at the electrodes or improperly amplifiers in the EEG can produce saturation or cutoff distortion, Fig B.5 depicts affects of saturation or cutoff distortion [6].

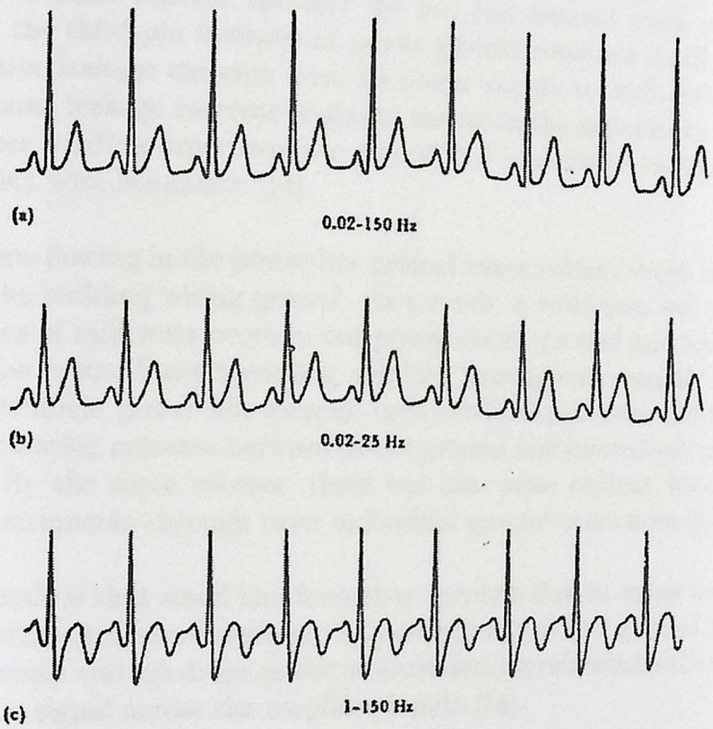


Figure B.5: Affects of saturation or cutoff distortion [6].

### Ground Loop

Ground loops can create seemingly intractable problems with line-frequency (50 or 60 Hz) interference in low-level biopotential recordings. They often occur when biopotential amplifiers are connected to signal processing or recording systems such as filters, oscilloscopes, or computer-based data acquisition systems. The root cause is often that the reference wires of signal cables interconnect the ground references of all the instruments, Fig B.6 de-

picts ground loop. However, each instrument is also referenced to a power line ground through its third-wire grounding pin on the power-line plug, as required by electrical safety codes [6][14].

Interference arises from the fact that all power grounds and signal-ground references are not equal. Line-powered instruments and appliances are only supposed to draw current through the hot and neutral wires of the line. However, the third-pin instrument power ground conducts small capacitive and resistive leakage currents from its power supply to wall-outlet ground. These ground leakage currents originate mostly in the instrument power-line transformer winding capacitance to ground and in resistive leakage from less than perfect wire insulation [14].

Currents flowing in the power-line ground cause voltage drops in the resistance of the building wiring ground. As a result, a voltmeter will often show several tens of millivolts between one power outlet ground and another even in the same room. Since recording amplifier grounds are usually referenced to the instrument power-line ground, millivolt-level potential differences can create circulating currents between power-ground and instrument-ground references. By the same process, there can also arise current flows between various instruments through their individual ground references [6][14][15].

The result is that small line-frequency currents flow in loops between different instruments interconnected by multiple signal and ground references. Line-frequency voltage drops in the interconnecting reference path wiring can appear as a signal across the amplifier inputs [14].

The ground loop can be eliminated by many solutions:

1. Use of isolation modules on the amplifier.

2. Earth grounding the amplifier input stages.

3. Using battery-powered equipment.

4. Connecting machines to the same ground and having only one connection to the patient.

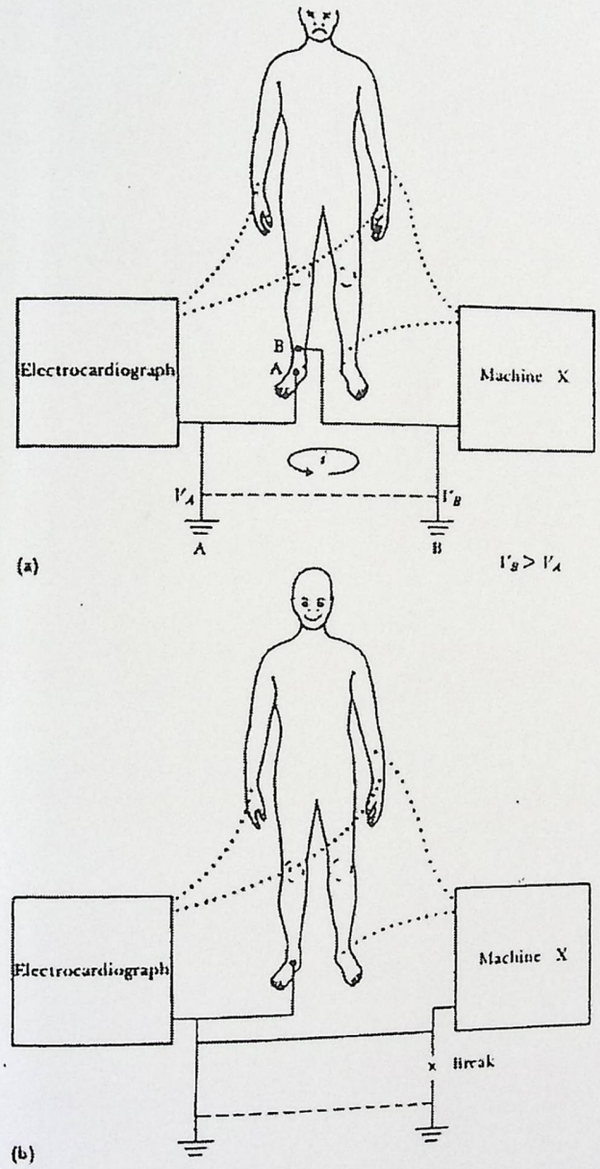


Figure B.6: Example of a ground loop between an ECG device and another electric machine connected to the same patient [6].

# Appendix C

# Three fold testing code

```
function [error_s1,error_r1,error_l1,error_s2,error_r2,error_l2,...
 error_s3,error_r3,error_l3] = best13(L,freq1,freq2,clustnum,statnum,leng)

% Returns errors of the silence, right and left.
% L is the length of each window.
% Range of frequencies between freq1 and freq2.
% leng is the length of the data in the decoding stage.
% Clustnum is the number of clusters which equal the number of symbols.
% statnum is the number of states.
% leng is the length of data during the evaluation stage.


data = load('data.mat');
silence = data.silence;
right = data.right;
left = data.left;

l = length(silence);
rws = l/L;


a = reshape(silence,L,rws)';
b = reshape(right,L,rws)';
c = reshape(left,L,rws)';
```

```
%DCT
for i = 1:rws
    a(i,:) = dct(a(i,:));
    b(i,:) = dct(b(i,:));
    c(i,:) = dct(c(i,:));
end

%Frequencies from 5 to 10 only.
aaa = a(:,freq1:freq2);
bbb = b(:,freq1:freq2);
ccc = c(:,freq1:freq2);

%Normalizing
for i = 1:rws
    maxaaa = max(aaa(i,:));
    minaaa = min(aaa(i,:));
    if(maxaaa~=minaaa)
        aaa(i,:) = aaa(i,:)/(maxaaa-minaaa);
    end

    maxbbb = max(bbb(i,:));
    minbbb = min(bbb(i,:));
    if(maxbbb~=minbbb)
        bbb(i,:) = bbb(i,:)/(maxbbb-minbbb);
    end

    maxccc = max(ccc(i,:));
    minccc = min(ccc(i,:));
    if(maxccc ~= minccc)
        ccc(i,:) = ccc(i,:)/(maxccc-minccc);
    end
end

portion = fix(rws/3);

% to make three folds we divide the number of rows into 3
```

```
clear left right silence data

Train = 2*portion;
Test = portion;


%Fold 1
%Data for training
silenceT = aaa(1:Train,:);
rightT = bbb(1:Train,:);
leftT = ccc(1:Train,:);

%Data for testing
silence = aaa(Train:rws,:);
right = bbb(Train:rws,:);
left = ccc(Train:rws,:);

data = [silenceT;rightT;leftT];
[center,U] = fcm(data,clustnum);
maxU = max(U);

for i = 1:clustnum
    index{i} = find(maxU == U(i,:));
    data(index{i},:)=i;
end

% Sequence of labels

data = data(:,1)';

clear silenceT leftT rightT

silenceT = data(1 : Train);
rightT = data(Train+1 : 2*Train);
leftT = data(2*Train+1 : 3*Train);
```

```
%Cluster the data for testing
newdata = [silence;right;left];
out = distfcm(center,newdata);
%We intrest in the minimum distance
minout = min(out);
for i = 1:clustnum
    index{i} = find(minout == out(i,:));
    newdata(index{i},:)=i;
end

newdata = newdata(:,1)';

clear silence right left
 silence = newdata(1 : Test);
 right = newdata(Test + 1 : 2*Test);
 left = newdata(2*Test + 1 : 3*Test);


%HMM
%2 states and 5 symbols
trs = normalise(rand(statnum),2);
es = normalise(rand(statnum,clustnum),2);
trr = normalise(rand(statnum),2);
er = normalise(rand(statnum,clustnum),2);
trl = normalise(rand(statnum),2);
el = normalise(rand(statnum,clustnum),2);
%Training
[trs,es] = hmmtrain(silenceT,trs,es);
[trr,er] = hmmtrain(rightT,trr,er);
[trl,el] = hmmtrain(leftT,trl,el);

error_s1 = 0;
error_r1 = 0;
error_l1 = 0;


for i = 1:leng:(Test-leng+1)
    [states, probability_o] = hmmdecode(silence(i:(i+leng-1)),trs,es);
```

```
    x = probability_o;
    [states, probability_o] = hmmdecode(right(i:(i+leng-1)),trr,er);
    y = probability_o;
    [states, probability_o] = hmmdecode(left(i:(i+leng-1)),trl,el);
    z = probability_o;

    % All combinations
    [states, probability_o1] = hmmdecode(left(i:(i+leng-1)),trs,es);
    [states, probability_o2] = hmmdecode(right(i:(i+leng-1)),trs,es);
    if(probability_o1>=x || probability_o2>=x)
        error_s1 = error_s1 + 1;
    end

    [states, probability_o1] = hmmdecode(silence(i:(i+leng-1)),trr,er);
    [states, probability_o2] = hmmdecode(left(i:(i+leng-1)),trr,er);
    if(probability_o1>=y || probability_o2>=y)
        error_r1 = error_r1 + 1;
    end

    [states, probability_o1] = hmmdecode(silence(i:(i+leng-1)),trl,el);
    [states, probability_o2] = hmmdecode(right(i:(i+leng-1)),trl,el);
    if(probability_o1>=z || probability_o2>=z)
        error_l1 = error_l1 + 1;
    end
end

error_s1 = error_s1/length(1:leng:(190-leng+1));
error_r1 = error_r1/length(1:leng:(190-leng+1));
error_l1 = error_l1/length(1:leng:(190-leng+1));

%END Fold 1



%Fold 2
%Data for training
silenceT = aaa(Test:rws,:);
```

```
rightT = bbb(Test:rws,:);
leftT = ccc(Test:rws,:);
%Data for testing
silence = aaa(1:Test,:);
right = bbb(1:Test,:);
left = ccc(1:Test,:);

data = [silenceT;rightT;leftT];
[center,U] = fcm(data,clustnum);
maxU = max(U);

for i = 1:clustnum
    index{i} = find(maxU == U(i,:));
    data(index{i},:)=i;
end

% Sequence of labels
data = data(:,1)';

clear silenceT leftT rightT

silenceT = data(1 : Train);
rightT = data(Train + 1 : 2*Train);
leftT = data(2*Train + 1: 3 * Train );

%Cluster the data for testing
newdata = [silence;right;left];
out = distfcm(center,newdata);
%We intrest in the minimum distance
minout = min(out);
for i = 1:clustnum
    index{i} = find(minout == out(i,:));
    newdata(index{i},:)=i;
end

newdata = newdata(:,1)';

clear silence right left
```

```
silence = newdata(1:Test);
right = newdata(Test + 1 : 2*Test);
left = newdata(2*Test + 1 : 3*Test);



%HMM
%2 states and 5 symbols
trs = normalise(rand(statnum),2);
es = normalise(rand(statnum,clustnum),2);
trr = normalise(rand(statnum),2);
er = normalise(rand(statnum,clustnum),2);
trl = normalise(rand(statnum),2);
el = normalise(rand(statnum,clustnum),2);
%Training
[trs,es] = hmmtrain(silenceT,trs,es);
[trr,er] = hmmtrain(rightT,trr,er);
[trl,el] = hmmtrain(leftT,trl,el);

error_s2 = 0;
error_r2 = 0;
error_l2 = 0;


for i = 1:leng:(Test-leng+1)
    [states, probability_o] = hmmdecode(silence(i:(i+leng-1)),trs,es);
    x = probability_o;   % Could be assumed as the threshold for Silence
    [states, probability_o] = hmmdecode(right(i:(i+leng-1)),trr,er);
    y = probability_o;
    [states, probability_o] = hmmdecode(left(i:(i+leng-1)),trl,el);
    z = probability_o;

    % All combinations
    [states, probability_o1] = hmmdecode(left(i:(i+leng-1)),trs,es);
    [states, probability_o2] = hmmdecode(right(i:(i+leng-1)),trs,es);
    if(probability_o1>=x || probability_o2>=x)
```

```
        error_s2 = error_s2 + 1;
    end

    [states, probability_o1] = hmmdecode(silence(i:(i+leng-1)),trr,er);
    [states, probability_o2] = hmmdecode(left(i:(i+leng-1)),trr,er);
    if(probability_o1>=y || probability_o2>=y)
        error_r2 = error_r2 + 1;
    end

    [states, probability_o1] = hmmdecode(silence(i:(i+leng-1)),trl,el);
    [states, probability_o2] = hmmdecode(right(i:(i+leng-1)),trl,el);
    if(probability_o1>=z || probability_o2>=z)
        error_l2 = error_l2 + 1;
    end
end

error_s2 = error_s2/length(1:leng:(190-leng+1));
error_r2 = error_r2/length(1:leng:(190-leng+1));
error_l2 = error_l2/length(1:leng:(190-leng+1));


half = fix(Train/2);
shalf = rws-half;

%Fold 3
%Data for training
silenceT = cat(1,aaa(1:half,:),aaa(shalf:rws,:));
rightT = cat(1,bbb(1:half,:),bbb(shalf:rws,:));
leftT = cat(1,ccc(1:half,:),ccc(shalf:rws,:));
%Data for testing
silence = aaa(half:shalf,:);
right = bbb(half:shalf,:);
left = ccc(half:shalf,:);

data = [silenceT;rightT;leftT];
[center,U] = fcm(data,clustnum);
maxU = max(U);
```

```
for i = 1:clustnum
    index{i} = find(maxU == U(i,:));
    data(index{i},:)=i;
end

% Sequence of labels
data = data(:,1)';

clear silenceT leftT rightT

silenceT = data(1:Train);
rightT = data(Train + 1 : 2*Train);
leftT = data(2*Train + 1 : 3*Train);

%Cluster the data for testing
newdata = [silence;right;left];
out = distfcm(center,newdata);
%We intrest in the minimum distance
minout = min(out);
for i = 1:clustnum
    index{i} = find(minout == out(i,:));
    newdata(index{i},:)=i;
end

newdata = newdata(:,1)';

clear silence right left
 silence = newdata(1:Test);
 right = newdata(Test + 1 : 2*Test );
 left = newdata(2*Test + 1 : 3*Test);




%HMM
%2 states and 5 symbols
trs = normalise(rand(statnum),2);
```

```
es = normalise(rand(statnum,clustnum),2);
trr = normalise(rand(statnum),2);
er = normalise(rand(statnum,clustnum),2);
trl = normalise(rand(statnum),2);
el = normalise(rand(statnum,clustnum),2);
%Training
[trs,es] = hmmtrain(silenceT,trs,es);
[trr,er] = hmmtrain(rightT,trr,er);
[trl,el] = hmmtrain(leftT,trl,el);

error_s3 = 0;
error_r3 = 0;
error_l3 = 0;


for i = 1:leng:(Test-leng+1)
    [states, probability_o] = hmmdecode(silence(i:(i+leng-1)),trs,es);
    x = probability_o;   % Could be assumed as the threshold for Silence
    [states, probability_o] = hmmdecode(right(i:(i+leng-1)),trr,er);
    y = probability_o;
    [states, probability_o] = hmmdecode(left(i:(i+leng-1)),trl,el);
    z = probability_o;

    % All combinations
    [states, probability_o1] = hmmdecode(left(i:(i+leng-1)),trs,es);
    [states, probability_o2] = hmmdecode(right(i:(i+leng-1)),trs,es);
    if(probability_o1>=x || probability_o2>=x)
        error_s3 = error_s3 + 1;
    end

    [states, probability_o1] = hmmdecode(left(i:(i+leng-1)),trr,er);
    [states, probability_o2] = hmmdecode(silence(i:(i+leng-1)),trr,er);
    if(probability_o1>=y || probability_o2>=y)
        error_r3 = error_r3 + 1;
    end

    [states, probability_o1] = hmmdecode(silence(i:(i+leng-1)),trl,el);
    [states, probability_o2] = hmmdecode(right(i:(i+leng-1)),trl,el);
```

```
    if(probability_o1>=z || probability_o2>=z)
        error_l3 = error_l3 + 1;
    end
end

error_s3 = error_s3/length(1:leng:(190-leng+1));
error_r3 = error_r3/length(1:leng:(190-leng+1));
error_l3 = error_l3/length(1:leng:(190-leng+1));
```

# Appendix D

# DAQ data sheet

This is the datasheet of PCI-6024E from National Instrument Company.

# Low-Cost E Series Multifunction DAQ – 12 or 16-Bit, 200 kS/s, 16 Analog Inputs

## NI E Series – Low-Cost

- 16 analog inputs at up to 200 kS/s, 12 or 16-bit resolution
- Up to 2 analog outputs at 10 kS/s, 12 or 16-bit resolution
- 8 digital I/O lines (TTL/CMOS); two 24-bit counter/timers
- Digital triggering
- 4 analog input signal ranges
- NI-DAQ driver that simplifies configuration and measurements

**Families**

- NI 6036E
- NI 6034E
- NI 6025E
- NI 6024E
- NI 6023E

**Operating Systems**

- Windows 2000/NT/XP
- Real-time performance with LabVIEW
- Others such as Linux® and Mac OS X

**Recommended Software**

- LabVIEW
- LabWindows/CVI
- Measurement Studio
- VI Logger

**Other Compatible Software**

- Visual Basic, C/C++, and C#

**Driver Software (included)**

- NI-DAQ 7

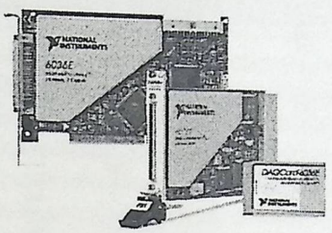

| Family | Bus | Analog Inputs | Input Resolution | Max Sampling Rate | Input Range | Analog Outputs | Output Resolution | Output Rate | Output Range | Digital I/O | Counter/Timers | Triggers |
|---|---|---|---|---|---|---|---|---|---|---|---|---|
| NI 6036E | PCI, PCMCIA | 16 SE/8 DI | 16 bits | 200 kS/s | ±0.05 to ±10 V | 2 | 16 bits | 10 kS/s[1] | ±10 V | 8 | 2, 24-bit | Digital |
| NI 6034E | PCI | 16 SE/8 DI | 16 bits | 200 kS/s | ±0.05 to ±10 V | 0 | – | – | – | 8 | 2, 24-bit | Digital |
| NI 6025E | PCI, PXI | 16 SE/8 DI | 12 bits | 200 kS/s | ±0.05 to ±10 V | 2 | 12 bits | 10 kS/s[1] | ±10 V | 8 | 2, 24-bit | Digital |
| NI 6024E | PCI, PCMCIA | 16 SE/8 DI | 12 bits | 200 kS/s | ±0.05 to ±10 V | 2 | 12 bits | 10 kS/s[1] | ±10 V | 8 | 2, 24-bit | Digital |
| NI 6023E | PCI | 16 SE/8 DI | 12 bits | 200 kS/s | ±0.05 to ±10 V | 0 | – | – | – | 8 | 2, 24-bit | Digital |

[1] 10 kS/s typical when using the single DMA channel for analog output. 1 kS/s maximum when using the single DMA channel for either analog input or counter/timer operations. 1 kS/s maximum for PCMCIA DAQCard devices in all cases

*Table 1. Low-Cost E Series Model Guide*

## Overview and Applications

National Instruments low-cost E Series multifunction data acquisition devices provide full functionality at a price to meet the needs of the budget-conscious user. They are ideal for applications ranging from continuous high-speed data logging to control applications to high-voltage signal or sensor measurements when used with NI signal conditioning. Synchronize the operations of multiple devices using the RTSI bus or PXI trigger bus to easily integrate other hardware such as motion control and machine vision to create an entire measurement and control system.

## Highly Accurate Hardware Design

NI low-cost E Series DAQ devices include the following features and technologies:

**Temperature Drift Protection Circuitry** – Designed with components that minimize the effect of temperature changes on measurements to less than 0.0010% of reading/°C.

**Resolution-Improvement Technologies** – Carefully designed noise floor maximizes the resolution.

**Onboard Self-Calibration** – Precise voltage reference included for calibration and measurement accuracy. Self-calibration is completely software controlled, with no potentiometers to adjust.

**NI DAQ-STC** – Timing and control ASIC designed to provide more flexibility, lower power consumption, and a higher immunity to noise and jitter than off-the-shelf counter/timer chips.

**NI MITE** – ASIC designed to optimize data transfer for multiple simultaneous operations using bus mastering with one DMA channel, interrupts, or programmed I/O.

**NI PGIA** – Measurement and instrument class amplifier that guarantees settling times at all gains. Typical commercial off-the-shelf amplifier components do not meet the settling time requirements for high-gain measurement applications.

**PFI Lines** – Eight programmable function input (PFI) lines that you can use for software-controlled routing of interboard and intraboard digital and timing signals.

**RTSI or PXI Trigger Bus** – Bus used to share timing and control signals between two or more PCI or PXI devices to synchronize operations.

**RSE Mode** – In addition to differential and nonreferenced single-ended modes, NI low-cost E Series devices offer the referenced single-ended (RSE) mode for use with floating-signal sources in applications with channel counts higher than eight.

**Onboard Temperature Sensor** – Included for monitoring the operating temperature of the device to ensure that it is operating within the specified range.

NATIONAL INSTRUMENTS

Figure D.1: Data sheet

| Models | | Full-Featured E Series | | | | Low-Cost E Series | | Basic |
|---|---|---|---|---|---|---|---|---|
| | | NI 6030E, NI 6031E, NI 6032E, NI 6033E | NI 6052E | NI 6070E, NI 6071E | NI 6040E | NI 6034E, NI 6036E | NI 6023E, NI 6024E, NI 6025E | PCI-6013, PCI-6014 |
| Measurement Sensitivity[1] (mV) | | 0.0023 | 0.0025 | 0.009 | 0.008 | 0.0036 | 0.008 | 0.004 |
| Nominal Range (V) | | | | | | | | |
| Positive FS | Negative FS | Absolute Accuracy (mV) | | | | | | |
| 10 | -10 | 1.147 | 4.747 | 14.389 | 15.373 | 7.560 | 16.504 | 8.984 |
| 5 | -5 | 2.077 | 0.876 | 5.193 | 5.697 | 1.790 | 5.263 | 2.003 |
| 2.5 | -2.5 | – | 1.190 | 3.605 | 3.859 | – | – | – |
| 2 | -2 | 0.836 | – | – | – | – | – | – |
| 1 | -1 | 0.422 | 0.479 | 1.452 | 1.556 | – | – | – |
| 0.5 | -0.5 | 0.215 | 0.243 | 0.735 | 0.789 | 0.399 | 0.846 | 0.471 |
| 0.25 | -0.25 | – | 0.137 | 0.379 | 0.405 | – | – | – |
| 0.2 | -0.2 | 0.102 | – | – | – | – | – | – |
| 0.1 | -0.1 | 0.061 | 0.064 | 0.163 | 0.176 | – | – | – |
| 0.05 | -0.05 | – | 0.035 | 0.091 | 0.100 | 0.0611 | 0.106 | 0.069 |
| 10 | 0 | 0.576 | 1.232 | 6.765 | 7.269 | – | – | – |
| 5 | 0 | 1.992 | 2.119 | 5.391 | 5.645 | – | – | – |
| 2 | 0 | 0.802 | 0.850 | 2.167 | 2.271 | – | – | – |
| 1 | 0 | 0.405 | 0.428 | 1.092 | 1.146 | – | – | – |
| 0.5 | 0 | 0.207 | 0.242 | 0.558 | 0.583 | – | – | – |
| 0.2 | 0 | 0.098 | 0.111 | 0.235 | 0.247 | – | – | – |
| 0.1 | 0 | 0.059 | 0.059 | 0.127 | 0.135 | – | – | – |

**Note:** Accuracies are valid for measurements following an internal calibration. Measurement accuracies are listed for operational temperatures within ±1 °C of internal calibration temperature and ±10 °C of external or factory-calibration temperature. One-year calibration interval recommended. The Absolute Accuracy at Full Scale calculations were performed for a maximum range input voltage (for example, 10 V for the ±10 V range) after one year, assuming 100 pt averaging of data.
[1]Smallest detectable voltage change in the input signal at the smallest input range.

*Table 2. E Series Analog Input Absolute Accuracy Specifications*

| Models | | Full-Featured E Series | | | | Low-Cost E Series | | Basic |
|---|---|---|---|---|---|---|---|---|
| | | NI 6030E, NI 6031E, NI 6032E, NI 6033E | NI 6052E | NI 6070E, NI 6071E | NI 6040E | NI 6034E, NI 6036E | NI 6023E, NI 6024E, NI 6025E | PCI-6013, PCI-6014 |
| Nominal Range (V) | | | | | | | | |
| Positive FS | Negative FS | Absolute Accuracy (mV) | | | | | | |
| 10 | -10 | 1.430 | 1.405 | 8.127 | 8.127 | 2.417 | 8.127 | 3.835 |
| 10 | 0 | 1.201 | 1.176 | 5.685 | 5.685 | – | – | – |

*Table 3. E Series Analog Output Absolute Accuracy Specifications*

## High-Performance, Easy-to-Use Driver Software

NI-DAQ is the robust driver software that makes it easy to access the functionality of your data acquisition hardware, whether you are a beginning or advanced user. Helpful features include:

**Automatic Code Generation** – DAQ Assistant is an interactive guide that steps you through configuring, testing, and programming measurement tasks and generates the necessary code automatically for NI LabVIEW, LabWindows/CVI, or Measurement Studio.

**Cleaner Code Development** – Basic and advanced software functions have been combined into one easy-to-use yet powerful set to help you build cleaner code and move from basic to advanced applications without replacing functions.

**High-Performance Driver Engine** – Software-timed single-point input (typically used in control loops) with NI-DAQ achieves rates of up to 50 kHz. NI-DAQ also delivers maximum I/O system throughput with a multithreaded driver.

**Test Panels** – With NI-DAQ, you can test all of your device functionality before you begin development.

**Scaled Channels** – Easily scale your voltage data into the proper engineering units using the NI-DAQ Measurement Ready virtual channels by choosing from a list of common sensors and signals or creating your own custom scale.

**LabVIEW Integration** – All NI-DAQ functions create the waveform data type, which carries acquired data and timing information directly into more than 400 LabVIEW built-in analysis routines for display of results in engineering units on a graph.

***For information on applicable hardware for NI-DAQ 7, visit* ni.com/dataacquisition.**

***Visit* ni.com/oem *for quantity discount information.***



Figure D.2: Data sheet

## Recommended Accessories

Signal conditioning is required for sensor measurements or voltage inputs greater than 10 V. National Instruments SCXI is a versatile, high-performance signal conditioning platform, intended for high-channel-count applications. NI SCC products provide portable, flexible signal conditioning options on a per-channel basis. Both signal conditioning platforms are designed to increase the performance and reliability of your DAQ system, and are up to 10 times more accurate than terminal blocks (please visit **ni.com/sigcon** for more details). Refer to the table below for more information:

**Sensor/Signals (>10 V)**

| System Description | DAQ Device | Signal Conditioning |
|---|---|---|
| High-performance | PCI-60xxE, PXI-60xxE, DAQCard-60xxE | SCXI |
| Low-cost, portable | PCI-60xxE, PXI-60xxE, DAQCard-60xxE | SCC |

**Signals (<10 V)[1]**

| System Description | DAQ Device | Terminal Block | Cable |
|---|---|---|---|
| Shielded | PCI-60xxE | SCB-68 | SH6868-EP |
| Shielded | PXI-60xxE | TB-2705 | SH6868-EP |
| Shielded | DAQCard-60xxE | SCB-68 | SHC6868-EP |
| Low-cost | PCI-6025E/PXI-6025E | Two TBX-68s | SH1006868 |
| Low-cost | PCI-60xxE/PXI-60xxE | CB-68LP | R6868 |
| Low-cost | DAQCard-60xxE | CB-68LP | RC6868 |

[1]Terminal blocks do not provide signal conditioning (i.e., filtering, amplification, isolation, and so on), which may be necessary to increase the accuracy of your measurements.

*Table 4. Recommended Accessories*

### Ordering Information

**PCI**

NI PCI-6036E ..... 778465-01
NI PCI-6034E ..... 778075-01
NI PCI-6025E ..... 777744-01
NI PCI-6024E ..... 777743-01
NI PCI-6023E ..... 777742-01

**PCMCIA**

NI DAQCard-6036E ..... 778561-01
NI DAQCard-6024E ..... 778269-01

**PXI**

NI PXI-6025E ..... 777798-01

Includes NI-DAQ driver software.

**BUY NOW!**

For complete product specifications, pricing, and accessory information, call (800) 813 3693 (U.S.) or go to ni.com/



Figure D.3: Data sheet

# Low Cost, Low Power Instrumentation Amplifier

# AD620

FEATURES
EASY TO USE
Gain Set with One External Resistor
(Gain Range 1 to 1000)
Wide Power Supply Range (±2.3 V to ±18 V)
Higher Performance than Three Op Amp IA Designs
Available in 8-Lead DIP and SOIC Packaging
Low Power, 1.3 mA max Supply Current

EXCELLENT DC PERFORMANCE ("B GRADE")
50 μV max, Input Offset Voltage
0.6 μV/°C max, Input Offset Drift
1.0 nA max, Input Bias Current
100 dB min Common-Mode Rejection Ratio (G = 10)

LOW NOISE
9 nV/√Hz, @ 1 kHz, Input Voltage Noise
0.28 μV p-p Noise (0.1 Hz to 10 Hz)

EXCELLENT AC SPECIFICATIONS
120 kHz Bandwidth (G = 100)
15 μs Settling Time to 0.01%

APPLICATIONS
Weigh Scales
ECG and Medical Instrumentation
Transducer Interface
Data Acquisition Systems
Industrial Process Controls
Battery Powered and Portable Equipment

CONNECTION DIAGRAM

8-Lead Plastic Mini-DIP (N), Cerdip (Q) and SOIC (R) Packages

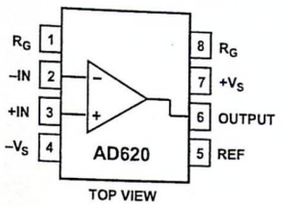


## PRODUCT DESCRIPTION

The AD620 is a low cost, high accuracy instrumentation amplifier that requires only one external resistor to set gains of 1 to 1000. Furthermore, the AD620 features 8-lead SOIC and DIP packaging that is smaller than discrete designs, and offers lower power (only 1.3 mA max supply current), making it a good fit for battery powered, portable (or remote) applications.

The AD620, with its high accuracy of 40 ppm maximum nonlinearity, low offset voltage of 50 μV max and offset drift of 0.6 μV/°C max, is ideal for use in precision data acquisition systems, such as weigh scales and transducer interfaces. Furthermore, the low noise, low input bias current, and low power of the AD620 make it well suited for medical applications such as ECG and noninvasive blood pressure monitors.

The low input bias current of 1.0 nA max is made possible with the use of Superβeta processing in the input stage. The AD620 works well as a preamplifier due to its low input voltage noise of 9 nV/√Hz at 1 kHz, 0.28 μV p-p in the 0.1 Hz to 10 Hz band, 0.1 pA/√Hz input current noise. Also, the AD620 is well suited for multiplexed applications with its settling time of 15 μs to 0.01% and its cost is low enough to enable designs with one in-amp per channel.

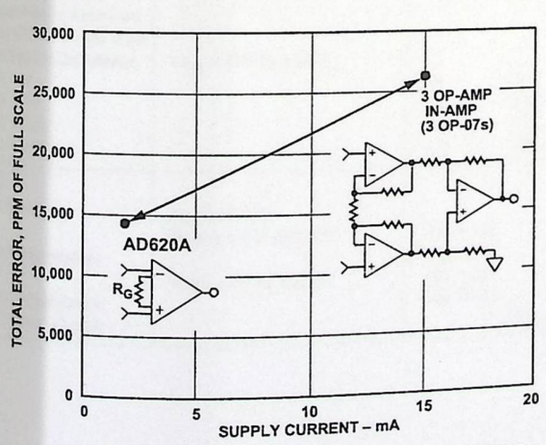


*Figure 1. Three Op Amp IA Designs vs. AD620*

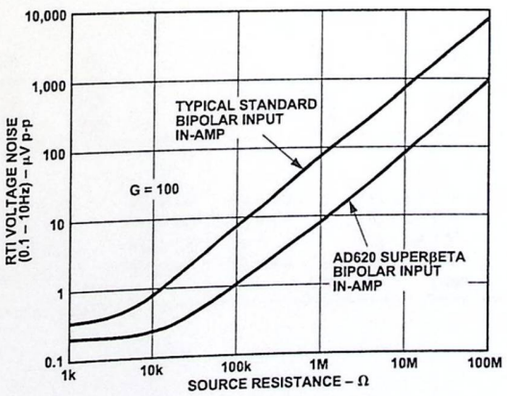


*Figure 2. Total Voltage Noise vs. Source Resistance*

REV. E



One Technology Way, P.O. Box 9106, Norwood, MA 02062-9106, U.S.A.
Tel: 781/329-4700 World Wide Web Site: http://www.analog.com
Fax: 781/326-8703

# AD620—SPECIFICATIONS

(Typical @ +25°C, $V_S$ = ±15 V, and $R_L$ = 2 kΩ, unless otherwise noted)

| Model | Conditions | AD620A Min | AD620A Typ | AD620A Max | AD620B Min | AD620B Typ | AD620B Max | AD620S[1] Min | AD620S[1] Typ | AD620S[1] Max | Units |
|---|---|---|---|---|---|---|---|---|---|---|---|
| GAIN | G = 1 + (49.4 k/$R_G$) | | | | | | | | | | |
| Gain Range | $V_{OUT}$ = ±10 V | 1 | | 10,000 | 1 | | 10,000 | 1 | | 10,000 | |
| Gain Error[2] | | | | | | | | | | | |
| G = 1 | | | 0.03 | 0.10 | | 0.01 | 0.02 | | 0.03 | 0.10 | % |
| G = 10 | | | 0.15 | 0.30 | | 0.10 | 0.15 | | 0.15 | 0.30 | % |
| G = 100 | | | 0.15 | 0.30 | | 0.10 | 0.15 | | 0.15 | 0.30 | % |
| G = 1000 | | | 0.40 | 0.70 | | 0.35 | 0.50 | | 0.40 | 0.70 | % |
| Nonlinearity, | $V_{OUT}$ = −10 V to +10 V, | | | | | | | | | | |
| G = 1–1000 | $R_L$ = 10 kΩ | | 10 | 40 | | 10 | 40 | | 10 | 40 | ppm |
| G = 1–100 | $R_L$ = 2 kΩ | | 10 | 95 | | 10 | 95 | | 10 | 95 | ppm |
| Gain vs. Temperature | G = 1 | | | | | | | | | | |
| | Gain >1[2] | | | 10 | | | 10 | | | 10 | ppm/°C |
| | | | | −50 | | | −50 | | | −50 | ppm/°C |
| VOLTAGE OFFSET | (Total RTI Error = $V_{OSI}$ + $V_{OSO}$/G) | | | | | | | | | | |
| Input Offset, $V_{OSI}$ | $V_S$ = ±5 V to ±15 V | | 30 | 125 | | 15 | 50 | | 30 | 125 | µV |
| Over Temperature | $V_S$ = ±5 V to ±15 V | | | 185 | | | 85 | | | 225 | µV |
| Average TC | $V_S$ = ±5 V to ±15 V | | 0.3 | 1.0 | | 0.1 | 0.6 | | 0.3 | 1.0 | µV/°C |
| Output Offset, $V_{OSO}$ | $V_S$ = ±15 V | | 400 | 1000 | | 200 | 500 | | 400 | 1000 | µV |
| | $V_S$ = ±5 V | | | 1500 | | | 750 | | | 1500 | µV |
| Over Temperature | $V_S$ = ±5 V to ±15 V | | | 2000 | | | 1000 | | | 2000 | µV |
| Average TC | $V_S$ = ±5 V to ±15 V | | 5.0 | 15 | | 2.5 | 7.0 | | 5.0 | 15 | µV/°C |
| Offset Referred to the Input vs. Supply (PSR) | $V_S$ = ±2.3 V to ±18 V | | | | | | | | | | |
| G = 1 | | 80 | 100 | | 80 | 100 | | 80 | 100 | | dB |
| G = 10 | | 95 | 120 | | 100 | 120 | | 95 | 120 | | dB |
| G = 100 | | 110 | 140 | | 120 | 140 | | 110 | 140 | | dB |
| G = 1000 | | 110 | 140 | | 120 | 140 | | 110 | 140 | | dB |
| INPUT CURRENT | | | | | | | | | | | |
| Input Bias Current | | | 0.5 | 2.0 | | 0.5 | 1.0 | | 0.5 | 2 | nA |
| Over Temperature | | | | 2.5 | | | 1.5 | | | 4 | nA |
| Average TC | | | 3.0 | | | 3.0 | | | 8.0 | | pA/°C |
| Input Offset Current | | | 0.3 | 1.0 | | 0.3 | 0.5 | | 0.3 | 1.0 | nA |
| Over Temperature | | | | 1.5 | | | 0.75 | | | 2.0 | nA |
| Average TC | | | 1.5 | | | 1.5 | | | 8.0 | | pA/°C |
| INPUT | | | | | | | | | | | |
| Input Impedance | | | | | | | | | | | |
| Differential | | | 10‖2 | | | 10‖2 | | | 10‖2 | | GΩ‖pF |
| Common-Mode | | | 10‖2 | | | 10‖2 | | | 10‖2 | | GΩ‖pF |
| Input Voltage Range[3] | $V_S$ = ±2.3 V to ±5 V | $-V_S$ + 1.9 | | $+V_S$ − 1.2 | $-V_S$ + 1.9 | | $+V_S$ − 1.2 | $-V_S$ + 1.9 | | $+V_S$ − 1.2 | V |
| Over Temperature | | $-V_S$ + 2.1 | | $+V_S$ − 1.3 | $-V_S$ + 2.1 | | $+V_S$ − 1.3 | $-V_S$ + 2.1 | | $+V_S$ − 1.3 | V |
| | $V_S$ = ±5 V to ±18 V | $-V_S$ + 1.9 | | $+V_S$ − 1.4 | $-V_S$ + 1.9 | | $+V_S$ − 1.4 | $-V_S$ + 1.9 | | $+V_S$ − 1.4 | V |
| Over Temperature | | $-V_S$ + 2.1 | | $+V_S$ − 1.4 | $-V_S$ + 2.1 | | $+V_S$ − 1.4 | $-V_S$ + 2.3 | | $+V_S$ − 1.4 | V |
| Common-Mode Rejection Ratio DC to 60 Hz with 1 kΩ Source Imbalance | $V_{CM}$ = 0 V to ±10 V | | | | | | | | | | |
| G = 1 | | 73 | 90 | | 80 | 90 | | 73 | 90 | | dB |
| G = 10 | | 93 | 110 | | 100 | 110 | | 93 | 110 | | dB |
| G = 100 | | 110 | 130 | | 120 | 130 | | 110 | 130 | | dB |
| G = 1000 | | 110 | 130 | | 120 | 130 | | 110 | 130 | | dB |
| OUTPUT | | | | | | | | | | | |
| Output Swing | $R_L$ = 10 kΩ, | | | | | | | | | | |
| | $V_S$ = ±2.3 V to ±5 V | $-V_S$ + 1.1 | | $+V_S$ − 1.2 | $-V_S$ + 1.1 | | $+V_S$ − 1.2 | $-V_S$ + 1.1 | | $+V_S$ − 1.2 | V |
| Over Temperature | | $-V_S$ + 1.4 | | $+V_S$ − 1.3 | $-V_S$ + 1.4 | | $+V_S$ − 1.3 | $-V_S$ + 1.6 | | $+V_S$ − 1.3 | V |
| | $V_S$ = ±5 V to ±18 V | $-V_S$ + 1.2 | | $+V_S$ − 1.4 | $-V_S$ + 1.2 | | $+V_S$ − 1.4 | $-V_S$ + 1.2 | | $+V_S$ − 1.4 | V |
| Over Temperature | | $-V_S$ + 1.6 | | $+V_S$ − 1.5 | $-V_S$ + 1.6 | | $+V_S$ − 1.5 | $-V_S$ + 2.3 | | $+V_S$ − 1.5 | V |
| Short Current Circuit | | | ±18 | | | ±18 | | | ±18 | | mA |

REV. E

| Model | Conditions | AD620A Min | AD620A Typ | AD620A Max | AD620B Min | AD620B Typ | AD620B Max | AD620S[1] Min | AD620S[1] Typ | AD620S[1] Max | Units |
|---|---|---|---|---|---|---|---|---|---|---|---|
| DYNAMIC RESPONSE | | | | | | | | | | | |
| Small Signal –3 dB Bandwidth | | | | | | | | | | | |
| G = 1 | | | 1000 | | | 1000 | | | 1000 | | kHz |
| G = 10 | | | 800 | | | 800 | | | 800 | | kHz |
| G = 100 | | | 120 | | | 120 | | | 120 | | kHz |
| G = 1000 | | | 12 | | | 12 | | | 12 | | kHz |
| Slew Rate | 10 V Step | 0.75 | 1.2 | | 0.75 | 1.2 | | 0.75 | 1.2 | | V/µs |
| Settling Time to 0.01% | | | | | | | | | | | |
| G = 1–100 | | | 15 | | | 15 | | | 15 | | µs |
| G = 1000 | | | 150 | | | 150 | | | 150 | | µs |
| NOISE | | | | | | | | | | | |
| Voltage Noise, 1 kHz | $Total\ RTI\ Noise = \sqrt{(e^2_{ni}) + (e_{no}/G)^2}$ | | | | | | | | | | |
| Input, Voltage Noise, $e_{ni}$ | | | 9 | 13 | | 9 | 13 | | 9 | 13 | nV/√Hz |
| Output, Voltage Noise, $e_{no}$ | | | 72 | 100 | | 72 | 100 | | 72 | 100 | nV/√Hz |
| RTI, 0.1 Hz to 10 Hz | | | | | | | | | | | |
| G = 1 | | | 3.0 | | | 3.0 | 6.0 | | 3.0 | 6.0 | µV p-p |
| G = 10 | | | 0.55 | | | 0.55 | 0.8 | | 0.55 | 0.8 | µV p-p |
| G = 100–1000 | | | 0.28 | | | 0.28 | 0.4 | | 0.28 | 0.4 | µV p-p |
| Current Noise | f = 1 kHz | | 100 | | | 100 | | | 100 | | fA/√Hz |
| 0.1 Hz to 10 Hz | | | 10 | | | 10 | | | 10 | | pA p-p |
| REFERENCE INPUT | | | | | | | | | | | |
| $R_{IN}$ | | | 20 | | | 20 | | | 20 | | kΩ |
| $I_{IN}$ | $V_{IN+}$, $V_{REF}$ = 0 | | +50 | +60 | | +50 | +60 | | +50 | +60 | µA |
| Voltage Range | | $-V_S + 1.6$ | | $+V_S - 1.6$ | $-V_S + 1.6$ | | $+V_S - 1.6$ | $-V_S + 1.6$ | | $+V_S - 1.6$ | V |
| Gain to Output | | | 1 ± 0.0001 | | | 1 ± 0.0001 | | | 1 ± 0.0001 | | |
| POWER SUPPLY | | | | | | | | | | | |
| Operating Range[4] | | ±2.3 | | ±18 | ±2.3 | | ±18 | ±2.3 | | ±18 | V |
| Quiescent Current | $V_S$ = ±2.3 V to ±18 V | | 0.9 | 1.3 | | 0.9 | 1.3 | | 0.9 | 1.3 | mA |
| Over Temperature | | | 1.1 | 1.6 | | 1.1 | 1.6 | | 1.1 | 1.6 | mA |
| TEMPERATURE RANGE | | | | | | | | | | | |
| For Specified Performance | | | –40 to +85 | | | –40 to +85 | | | –55 to +125 | | °C |

NOTES

[1]See Analog Devices military data sheet for 883B tested specifications.

[2]Does not include effects of external resistor $R_G$.

[3]One input grounded. G = 1.

[4]This is defined as the same supply range which is used to specify PSR.

Specifications subject to change without notice.

ANALOG DEVICES

# Ultralow Offset Voltage Operational Amplifiers

## OP07

### FEATURES

Low $V_{OS}$: 75 µV Max
Low $V_{OS}$ Drift: 1.3 µV/°C Max
Ultra-Stable vs. Time: 1.5 µV/Month Max
Low Noise: 0.6 µV p-p Max
Wide Input Voltage Range: ±14 V
Wide Supply Voltage Range: 3 V to 18 V
Fits 725,108A/308A, 741, AD510 Sockets
125°C Temperature-Tested Dice

### PIN CONNECTIONS

Epoxy Mini-Dip (P-Suffix)
8-Pin SO (S-Suffix)

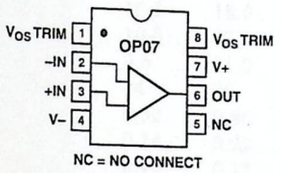


NC = NO CONNECT

### APPLICATIONS

Wireless Base Station Control Circuits
Optical Network Control Circuits
Instrumentation
Sensors and Controls
  Thermocouples
  RTDs
  Strain Bridges
  Shunt Current Measurements
Precision Filters

### GENERAL DESCRIPTION

The OP07 has very low input offset voltage (75 µV max for OP07E) which is obtained by trimming at the wafer stage. These low offset voltages generally eliminate any need for external nulling. The OP07 also features low input bias current (±4 nA for OP07E) and high open-loop gain (200 V/mV for OP07E). The low offsets and high open-loop gain make the OP07 particularly useful for high-gain instrumentation applications.

The wide input voltage range of ±13 V minimum combined with high CMRR of 106 dB (OP07E) and high input impedace provides high accuracy in the noninverting circuit configuration. Excellent linearity and gain accuracy can be maintained even at high closed-loop gains. Stability of offsets and gain with time or variations in temperature is excellent. The accuracy and stability of the OP07, even at high gain, combined with the freedom from external nulling have made the OP07 an industry standard for instrumentation applications.

The OP07 is available in two standard performance grades. The OP07E is specified for operation over the 0°C to 70°C range, and OP07C over the –40°C to +85°C temperature range.

The OP07 is available in epoxy 8-lead Mini-DIP and 8-lead SOIC. It is a direct replacement for 725,108A, and OP05 amplifiers; 741-types may be directly replaced by removing the 741's nulling potentiometer. For improved specifications, see the OP177 or OP1177. For ceramic DIP and TO-99 packages and standard micro circuit (SMD) versions, see the OP77.

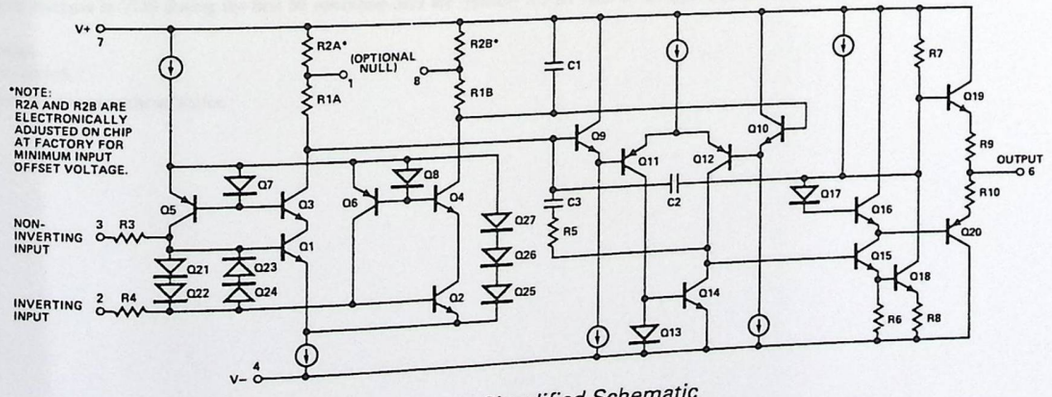


*Figure 1. Simplified Schematic*

REV. A



One Technology Way, P.O. Box 9106, Norwood, MA 02062-9106, U.S.A.
Tel: 781/329-4700
Fax: 781/326-8703
www.analog.com

# OP07–SPECIFICATIONS

## OP07E ELECTRICAL CHARACTERISTICS ($V_S$ = ±15 V, $T_A$ = 25°C, unless otherwise noted.)

| Parameter | Symbol | Conditions | Min | Typ | Max | Unit |
|---|---|---|---|---|---|---|
| INPUT CHARACTERISTICS | | | | | | |
| Input Offset Voltage[1] | $V_{OS}$ | | | 30 | 75 | μV |
| Long-Term $V_{OS}$ Stability[2] | $V_{OS}$/Time | | | 0.3 | 1.5 | μV/Mo |
| Input Offset Current | $I_{OS}$ | | | 0.5 | 3.8 | nA |
| Input Bias Current | $I_B$ | | | ±1.2 | ±4.0 | nA |
| Input Noise Voltage | $e_n$ p-p | 0.1 Hz to 10 Hz[3] | | 0.35 | 0.6 | μV p-p |
| Input Noise Voltage Density | $e_n$ | $f_O$ = 10 Hz | | 10.3 | 18.0 | $nV\sqrt{Hz}$ |
| | | $f_O$ = 100 Hz[3] | | 10.0 | 13.0 | $nV\sqrt{Hz}$ |
| | | $f_O$ = 1 kHz | | 9.6 | 11.0 | $nV\sqrt{Hz}$ |
| Input Noise Current | $I_n$ p-p | | | 14 | 30 | pA p-p |
| Input Noise Current Density | $I_n$ | $f_O$ = 10 Hz | | 0.32 | 0.80 | $pA\sqrt{Hz}$ |
| | | $f_O$ = 100 Hz[3] | | 0.14 | 0.23 | $pA\sqrt{Hz}$ |
| | | $f_O$ = 1 kHz | | 0.12 | 0.17 | $pA\sqrt{Hz}$ |
| Input Resistance—Differential Mode[4] | $R_{IN}$ | | 15 | 50 | | mΩ |
| Input Resistance—Common-Mode | $R_{INCM}$ | | | 160 | | GΩ |
| Input Voltage Range | IVR | | ±13 | ±14 | | V |
| Common-Mode Rejection Ratio | CMRR | $V_{CM}$ = ±13 V | 106 | 123 | | dB |
| Power Supply Rejection Ratio | PSRR | $V_S$ = ±3 V to ±18 V | | 5 | 20 | μV/V |
| Large-Signal Voltage Gain | $A_{VO}$ | $R_L \geq 2$ kΩ, $V_O$ = ±10 V | 200 | 500 | | V/mV |
| | | $R_L \geq 500$ Ω, $V_O$ = ±0.5 V, $V_S$ = ±3 V[4] | 150 | 400 | | V/mV |
| OUTPUT CHARACTERISTICS | | | | | | |
| Output Voltage Swing | $V_O$ | $R_L \geq 10$ kΩ | ±12.5 | ±13.0 | | V |
| | | $R_L \geq 2$ kΩ | ±12.0 | ±12.8 | | V |
| | | $R_L \geq 1$ kΩ | ±10.5 | ±12.0 | | V |
| DYNAMIC PERFORMANCE | | | | | | |
| Slew Rate | SR | $R_L \geq 2$ kΩ[3] | 0.1 | 0.3 | | V/μs |
| Closed-Loop Bandwidth | BW | $A_{VOL}$ = 1[5] | 0.4 | 0.6 | | MHz |
| Closed-Loop Output Resistance | $R_O$ | $V_O$ = 0, $I_O$ = 0 | | 60 | | Ω |
| Power Consumption | $P_d$ | $V_S$ = ±15 V, No Load | | 75 | 120 | mW |
| | | $V_S$ = ±13 V, No Load | | 4 | 6 | mW |
| Offset Adjustment Range | | $R_P$ = 20 kΩ | | ±4 | | mV |

NOTES

[1]Input offset voltage measurements are performed by automated test equipment approximately 0.5 seconds after application of power.

[2]Long-term input offset voltage stability refers to the averaged trend time of VOS vs. Time over extended periods after the first 30 days of operation. Excluding the initial hour of operation, changes in VOS during the first 30 operating days are typically 2.5 μV refer to the typical performance curves. Parameter is sample tested.

[3]Sample tested.

[4]Guaranteed by design.

[5]Guaranteed but not tested.

Specifications subject to change without notice.